

282. Finegan, J. D., *AEC Tech. Rept.* 15, Case Institute, Cleveland, Ohio, 1961.
283. Schroder, H., and G. M. Schmidt, *Z. Angew. Phys.*, **18**, 124 (1964).
284. Kloholm, E., *IBM Res. Rept.* RC 1508, 1965.
285. Wilcock, J. D., and D. S. Campbell, private communication.
286. Marsh, D. M., *J. Sci. Inst.*, **38**, 229 (1961).
287. Holland, L., T. Putner, and R. Ball, *Brit. J. Appl. Phys.*, **11**, 167 (1960).
288. Novice, M. A., *Vacuum*, **14**, 385 (1964).
289. Priest, J., H. L. Caswell, and Y. Budo, *Trans. 9th Natl. Vacuum Symp.*, 1962, p. 121.
290. Budo, Y., and J. Priest, *Solid-State Electron.*, **6**, 159 (1963).
291. Wilman, H., *Proc. Phys. Soc. London*, **N:68**, 474 (1955).
292. Hoffman, R. W., and H. S. Story, *J. Appl. Phys.*, **27**, 193 (1956).
293. Gafner, G., *Phil. Mag.*, **5**, 1041 (1960).
294. Buckel, W., *Z. Physik*, **133**, 136 (1954).
295. Finegan, J. D., and R. W. Hoffman, *AEC Tech. Rept.* 18, Case Institute, Cleveland, Ohio, 1961.
296. Buckel, W., in C. A. Neugebauer, J. B. Newkirk, and D. A. Vermilyea (eds.), "Structure and Properties of Thin Films," p. 53, John Wiley & Sons, Inc., New York, 1959.
297. Oswald, W., *Z. Phys. Chem.*, **22**, 289 (1879).
298. Grigson, C. W., and D. B. Dove, *J. Vacuum Sci. Technol.*, **3**, 120 (1966).
299. Dove, D. B., *J. Appl. Phys.*, **35**, 2785 (1964).
300. Hill, R. M., *Nature*, **204**, 35 (1964).
301. Shuttleworth, R., *Proc. Phys. Soc. London*, **A63**, 444 (1950).
302. Benson, G. C., and K. S. Yun, *J. Chem. Phys.*, **42**, 3085 (1965).
303. Piuz, F., and R. Ghez, *Helv. Phys. Acta*, **35**, 507 (1962).
304. McRae, E. G., and C. W. Caldwell, in H. C. Gatos (ed.), "Solid Surfaces," p. 509, North Holland Publishing Company, Amsterdam, 1964.
305. Van der Merwe, J. H., *J. Appl. Phys.*, **34**, 117 (1963).
306. Van der Merwe, J. H., in "Basic Problems in Thin Film Physics," p. 122, R. Niedermayer and H. Mayer (eds.), Vandenhoeck and Ruprecht, Goettingen, 1966.
307. Mathews, J. W., *Phil. Mag.*, **6**, 1347 (1961).
308. Mathews, J. W., *Phil. Mag.*, **13**, 1207 (1966).
309. Cabrera, N., *Mem., Sci. Rev. Metallurg.*, **62**, 205 (1965).
310. Neugebauer, C. A., *J. Appl. Phys.*, **31**, 1096 (1960).
311. Blakely, J. M., *J. Appl. Phys.*, **35**, 1756 (1964).
312. Rudakov, A. P., and N. A. Semenov, *Polymer Mech.*, **1**, 112 (1965).
313. Read, H. J., *Proc. Am. Electroplaters Soc.*, **50**, 37 (1963).
314. Angus, H. C., *Trans. Inst. Metal Finishing*, **39**, 30 (1962).
315. Palatnik, L. S., and A. I. Ll'inskii, *Soviet Phys. Solid State*, **3**, 2053 (1962).
316. Palatnik, L. S., G. V. Fedorov, and A. I. Ll'inskii, *Phys. Met. Metallog.*, **5**, 159 (1961).
317. Raffalovich, A. J., *Rev. Sci. Inst.*, **37**, 368 (1966).
318. Angus, H. G., *Brit. Appl. Phys.*, **13**, 58 (1962).
319. Branson Instrument, Inc., and Dawe Inst., Ltd., *Ultrasonics*, **4**, 88 (1966).
320. Menter, J. W., and D. W. Pashley, in C. A. Neugebauer, J. D. Newkirk, and D. A. Vermilyea (eds.), "Structure and Properties of Thin Films," p. 111, John Wiley & Sons, Inc., New York, 1959.
321. Neugebauer, C. A., in G. Hass and R. E. Thun (eds.), "Physics of Thin Films," vol. 2, p. 1, Academic Press Inc., New York, 1964.
322. Machlin, E. S., in "Strengthening Mechanisms in Solids," p. 375, American Society for Metals, Metals Park, Ohio, 1960.
323. Bilby, B. A., *Nature*, **182**, 296 (1958).
324. Campbell, D. S., in J. C. Anderson (ed.), "The Use of Thin Films in Physical Investigations," p. 299, Academic Press Inc., New York, 1966.
325. Grunes, R. L., C. D. D'Antonio, and F. Kiess, *J. Appl. Phys.*, **36**, 2735 (1965).
326. Jovanovic, S., and C. S. Smith, *J. Appl. Phys.*, **32**, 121 (1961).
327. D'Antonio, C., J. Hirshhorn, and L. Tarshis, *Trans. AIME*, **227**, 1346 (1963).

Chapter **13****Electrical Properties of  
Metallic Thin Films**

LEON I. MAISSEL

IBM Components Division, East Fishkill, New York

<b>1. Sources of Resistivity in Metallic Conductors</b> . . . . .	<b>13-2</b>
a. Temperature . . . . .	13-2
b. Point Defects . . . . .	13-3
c. Structural Imperfections . . . . .	13-4
d. Matthiessen's Rule . . . . .	13-4
<b>2. Commonly Measured Quantities for Thin Films</b> . . . . .	<b>13-5</b>
a. Sheet Resistance . . . . .	13-5
b. Measurement of Sheet Resistance . . . . .	13-5
c. Temperature Coefficient of Resistance (TCR) . . . . .	13-7
<b>3. Influence of Thickness on the Resistivity of a Structurally Perfect Film</b> . . . . .	<b>13-7</b>
a. Theory . . . . .	13-7
b. Experimental Results . . . . .	13-11
<b>4. Hall Effect and Magnetoresistance in Thin Films</b> . . . . .	<b>13-13</b>
<b>5. Negative Temperature Coefficients of Resistance in Films</b> . . . . .	<b>13-15</b>
a. Discontinuous Films . . . . .	13-15
b. Theories of Conduction in Discontinuous Films . . . . .	13-18
(1) Transport by Thermionic Emission . . . . .	13-18
(2) Transport by Activated-charge-carrier Creation and Tunneling . . . . .	13-18
(3) Transport by Tunneling between Allowed States . . . . .	13-19
(4) Transport by Substrate-assisted Tunneling . . . . .	13-20
(5) Other Models . . . . .	13-21
(6) Range of Applicability of Various Models . . . . .	13-22
c. Continuous Films . . . . .	13-22
<b>6. High-frequency Characteristics of Thin Films</b> . . . . .	<b>13-23</b>
<b>7. Influence of Heat Treatment</b> . . . . .	<b>13-26</b>
a. Annealing . . . . .	13-26
b. Agglomeration and Oxidation . . . . .	13-30
<b>References</b> . . . . .	<b>13-31</b>

## 1. SOURCES OF RESISTIVITY IN METALLIC CONDUCTORS

### a. Temperature

According to modern quantum electronic theory, electrical conduction in metals is due to electrons, while electrical resistivity results from the scattering of these electrons by the lattice. Because of their wave nature, electrons can pass through a perfect lattice without any attenuation (resistivity being, therefore, a measure of the extent to which a metal lattice departs from perfect regularity). Actually, no lattice is perfect. Electrons always undergo some scattering as they move through a solid, the average distance that they travel between collisions being called the mean free path.<sup>1,2</sup>

Even a lattice which has no structural defects or foreign atoms cannot be completely regular at any temperature, since the atoms will not be fixed (stationary) but will be vibrating about their mean positions. In considering interactions between the electrons and the various vibrational modes of the lattice (phonons), it is convenient to make use of the Debye temperature. In Debye's theory of specific heats, a crystal is assumed to possess a wide spectrum of vibrational modes, with a fixed upper limit. This is so because the minimum phonon wavelength must be of the order of atomic spacing. The Debye temperature  $\theta$  is then defined in terms of this maximum frequency by

$$\theta = \frac{h\nu_{\max}}{k}$$

where  $k$  is Boltzmann's constant.

At low temperatures ( $T \ll \theta$ ), resistivity varies as  $T^n$  (where  $n$  is close to 5), whereas at high temperatures ( $T \gg \theta$ ), resistivity varies linearly with  $T$ .

For many metals, the Debye temperature falls close to or below room temperature, so that the temperature variation of resistance above 25°C is approximately linear. This makes it possible to define a temperature coefficient of resistance  $\alpha$  which can be measured between two temperatures that are not extremely close together (see Sec. 2c):

$$\alpha = \frac{1}{R} \frac{\Delta R}{\Delta T} \quad (1)$$

The relationship between  $\alpha$  and the temperature dependence of the mean free path is shown in Table 1.

TABLE 1 Electronic Mean Free Path of Several Metals

Metal	Calculated mean free path, Å			Temp coeff ppm/°C (0-100)	Room temp resistivity, $\mu\text{ohm-cm}$
	-200°C	0°C	100°C		
Li.....	955	113	79	4,220	8.55
Na.....	1,870	335	233	4,400	4.3
K.....	1,330	376	240	5,500	6.1
Cu.....	2,965	421	294	4,330	1.69
Ag.....	2,425	575	405	4,100	1.47
Au.....	1,530	406	290	4,000	2.44
Ni.....	.....	133	80	6,750	7.24
Co.....	.....	130	79	6,580	9.7
Fe.....	2,785	220	156	4,110	8.85
Pt.....	720	110	79	3,920	9.83

### b. Point Defects

An impurity atom dissolved in a metal will, in general, carry an effective electric charge different from that of the parent metal; it will therefore serve as a source of electron scattering. Even if both the solvent and the solute have the same valence, the screening of the impurity ions by the electron gas will not be quite the same as that given to the parent ions, so that their effective charge will be slightly different. The same general picture holds for a vacancy or an interstitial. As might be expected, resistivity rises with increasing impurity concentration, reaching a maximum for an alloy composition of approximately 50% "impurity." Figure 1 illustrates this for the silver-gold system. The data are taken from Ref. 3.

A striking confirmation of the fact that electrical resistivity is a measure of the irregularity of the lattice is seen in the case of those alloys in which the impurity atoms can assume an ordered arrangement (or superlattice) within the host lattice. An

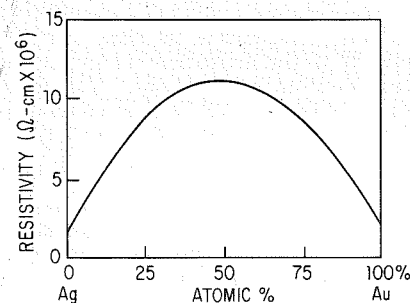


Fig. 1 Resistivity vs. composition for the gold-silver system.

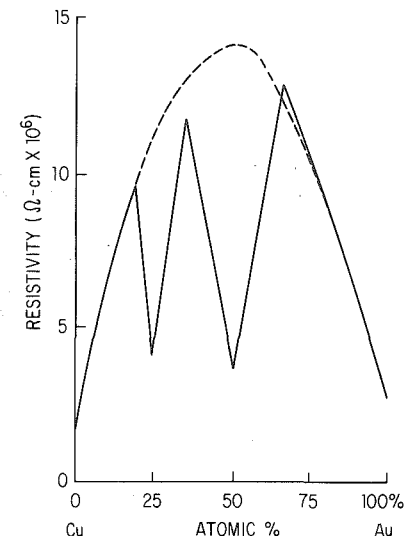


Fig. 2 Resistivity vs. composition for the gold-silver system, both quenched and annealed.

example of such a system is copper-gold. Figure 2 shows the resistivity vs. composition diagram for this system.<sup>3</sup> The solid line is for specimens that were annealed at 200°C to allow ordering to take place, whereas the dotted one is for specimens in which a random impurity distribution has been "frozen in" by quenching at 650°C.

As can be seen from these examples, impurities having the same number of valence electrons as the host increase the resistivity of the latter by a factor of about 0.1 per atomic percent impurity added, giving a maximum increase of a factor of 5 or so.

When the impurity atom has a valence different from that of the host, its effect on the resistivity is, understandably, considerably more pronounced. Contributions have been seen that are as high as a factor of 10 (increase) per atomic percent of impurity added.<sup>4</sup> However, impurities of this sort also cause extensive distortion of the lattice, so that in practice their solid solubility is severely limited. Thus, in bulk materials, resistivity increases due to dissolved impurities will not be much greater than by a factor of 10. In films, however, a considerably greater concentration of impurities than the equilibrium value may be trapped during deposition. As a result, increases in resistivity by factors of several hundred or more are often seen.

In addition, the high resistivities often seen in films prepared under poor deposition conditions may be due to the formation of an insulating phase which is randomly distributed throughout the film. An example of the transition from a dissolved impurity to an insulating phase, and its effect on resistivity, is shown in Fig. 3, taken from Ref. 5.

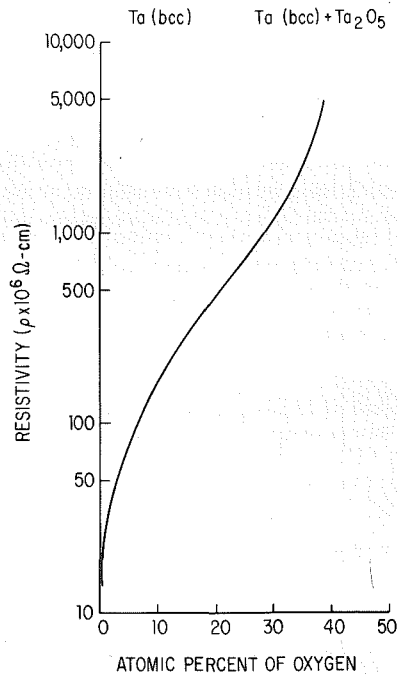


Fig. 3 Resistivity of tantalum as a function of oxygen impurity concentration.

### c. Structural Imperfections

The contributions to the resistivity made by vacancies and interstitials have been summarized by Damask and Dienes.<sup>6</sup> Typical values are of the order of  $1 \mu\text{ohm-cm}$  per atomic percent of vacancies or interstitials, although values as high as  $5.9 \mu\text{ohm-cm}$  per atomic percent of vacancies<sup>7</sup> and  $10.5 \mu\text{ohm-cm}$  per atomic percent of interstitials<sup>8</sup> have been recorded.

The scattering power of dislocations in metals is thought to be small.<sup>9</sup> For example, the contribution to the residual resistivity per dislocation per  $\text{cm}^2$  has been estimated<sup>10</sup> to be  $2.3 \times 10^{-13} \mu\text{ohm-cm}$ . This means that it takes a dislocation density of about  $10^{12}$  per  $\text{cm}^2$  to have the same effect as 1% of dissolved chemical impurity.

In general, a solid in equilibrium at absolute temperature  $T$  will have a concentration of imperfections in the order of  $e^{-W/kT}$ , where  $W$  is the activation energy for the formation of the imperfections. This corresponds to less than  $10^{-4}\%$  at room temperature for a  $W$  of about 1 eV. Much larger concentrations can be "frozen in" by quenching from high temperatures; but, even so, the equilibrium temperature for a concentration of as little as 1% is about  $3,000^\circ\text{K}$ .

The effect of grain boundaries on the resistivity of a bulk metal is, like that of dislocations, relatively small. This is not surprising since grain boundaries can be treated as a linear array of dislocations. As the size of the grains becomes smaller (and, hence, the role of the grain boundaries becomes more important), the material begins to resemble an amorphous solid—not too far removed in structure from that of a liquid. Thus, an estimate of the maximum possible contribution to the resistivity from grain boundaries may be arrived at by considering the resistivities of liquid metals. In general, the increase in resistivity due to melting is of the order of 5 to  $20 \mu\text{ohm-cm}$ . However, this is influenced by factors other than simply the change in grain-boundary density, as is evidenced by the fact that certain metals such as Ga, Sb, and Bi actually have lower resistivities in the liquid state than in the solid. We may also remark that thin films of sufficient thickness prepared under conditions of clean vacuum exhibit resistivities within a few percent of the bulk value despite having grain sizes in the order of only a few hundred angstroms.

It was mentioned above that an insulating phase may be present if sufficient impurities are trapped. It is frequently the case that such phases are concentrated at the grain boundaries. Under these circumstances, the role of the latter is entirely different. Some of these cases will be considered later.

### d. Matthiessen's Rule

As indicated above, electrical resistance in metals may arise from a variety of causes, such as temperature, dissolved impurities, and vacancies. Matthiessen's rule states that the resistivity of a given sample will be the simple arithmetic sum of the individual contributions made by all these separate sources of resistance. It is generally convenient to combine all the contributions to the resistivity, other than that of temperature, into one which is referred to as the residual resistivity.

$$\rho = \rho_{\text{temp}} + \rho_{\text{residual}}$$

Experimentally, Matthiessen's rule has been found to hold very well for bulk materials, and although careful measurements<sup>11</sup> have shown some deviation from it, the deviation is small enough to be neglected in most instances.<sup>1</sup>

Since the temperature coefficient of resistance is

$$\alpha = \frac{1}{\rho} \frac{d\rho}{dT} = \frac{1}{\rho} \frac{d\rho_{\text{temp}}}{dT}$$

it follows that

$$\alpha\rho = \frac{d\rho_{\text{temp}}}{dT} = \text{const} \quad (2)$$

Since both  $\alpha$  and  $\rho$  are usually known for the bulk, Eq. (2) is a particularly useful form of Matthiessen's rule. It is apparent that, as  $\rho$  becomes larger,  $\alpha$  will approach zero. Note, however, that (in terms of Matthiessen's rule)  $\alpha$  can never become negative.

Matthiessen's rule is useful in situations in which it is easier to measure the temperature coefficient of resistance than the resistivity. This could occur because of problems of accurate thickness measurement—for example, for films on nonplanar substrates. If the temperature coefficient of resistance is positive and exceeds a few hundred parts per million per  $^\circ\text{C}$ , we can assume that Matthiessen's rule will hold and Eq. (2) can be applied and the resistivity deduced. Experimental confirmation that Matthiessen's rule can hold even for very thin films has been given by Altman<sup>12</sup> for tantalum down to  $200 \text{ \AA}$  and by Young and Lewis<sup>13</sup> for chromium down to  $30 \text{ \AA}$ . Note that in both cases the electron mean free path was substantially less than the thickness of the film. Situations where this may not be the case will be discussed presently.

## 2. COMMONLY MEASURED QUANTITIES FOR THIN FILMS

### a. Sheet Resistance

As can be seen from Fig. 4, the resistance of a rectangularly shaped section of film (measured in a direction parallel to the film surface) is given by

$$R = \frac{\rho l}{d b} \quad (3)$$

If  $l = b$ , this then becomes

$$R = \frac{\rho}{d} = R_s$$

so that the resistance  $R_s$  of one square of film is independent of the size of the square—depending only on resistivity and thickness.

The quantity  $R_s$  is called the "sheet resistance" of the film and is expressed in ohms per square. It is a very useful quantity that is widely used for comparing films, particularly those of the same material deposited under similar conditions. If the thickness is known, the resistivity is readily obtained from

$$\rho = dR_s$$

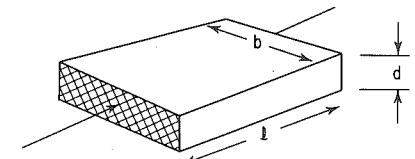


Fig. 4 Definition of sheet resistance.

### b. Measurement of Sheet Resistance

The most direct method of measuring  $R_s$  is to prepare a rectangular sample of film as shown in Fig. 5a, measure its resistance, and divide by the number of squares of film material that lie between the end contacts (four in our example). Where contact resistance between the film and the end terminals may be a problem, a four-terminal method is necessary (see Fig. 5b), the number of squares now being counted between

the two voltage terminals (five in this example), and  $R = V/I$ . It is advisable to make the voltage terminals as narrow as possible at their points of intersection with the film in order to reduce any uncertainty in counting the number of squares lying between them.

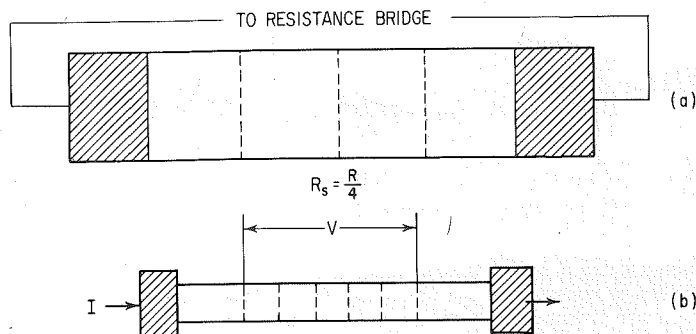


Fig. 5 Direct measurement of sheet resistance.

While direct measurement of the number of squares is the simplest method, a technique which does not call for the fabrication of a special sample for each determination of sheet resistance is usually preferred. Furthermore, it may be necessary to measure the variation of sheet resistance in a film from one part of the substrate to another, and the fabrication and measurement of a large number of tiny rectangles become highly impractical (in addition to being a destructive technique). Accordingly, widespread use is made of four-point-probe methods. The most common form of four-point probe is the in-line type illustrated schematically in Fig. 6.

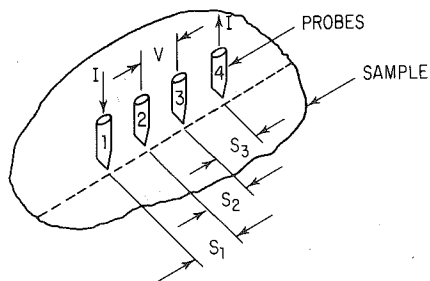


Fig. 6 In-line four-point probe.

This configuration has been treated in detail by Valdes,<sup>14</sup> who showed that when the probes are placed on a material of semi-infinite volume, the resistivity is given by

$$\rho = \frac{V}{I} \frac{2\pi}{1/s_1 + 1/s_3 - 1/(s_1 + s_2) - 1/(s_2 + s_3)}$$

When  $s_1 = s_2 = s_3 = s$ , this reduces to

$$\rho = \frac{V}{I} 2\pi s \quad (4)$$

If the material on which the probes are placed is an infinitely thin slice resting on an insulating support, it can be shown<sup>14</sup> that Eq. (4) becomes

$$\rho = \frac{V d\pi}{I \ln 2}$$

or

$$\frac{\rho}{d} = R_s = 4.532 \frac{V}{I} \quad (5)$$

Although Eq. (5) is independent of the probe spacing, the resolution of any particular probe will, of course, depend on spacing. Thus, a probe of spacing  $S$  centrally

located inside a square of film measuring  $6S \times 6S$  will give a reading that is about 20% too high if the square is surrounded by an insulating film and about 10% too low if it is surrounded by a film of infinite conductivity. For more exact corrections (to allow for edge effects) the reader is referred to Refs. 14 and 15. A number of four-point-probe assemblies are commercially available, being extensively used in the semiconductor industry. Probe spacings of 25 mils are commonly employed for routine use, whereas for high-resolution work, less robust models with spacings down to 10 mils are available.

In cases where very high resolution is needed, a square-probe array such as shown in Fig. 7 rather than a linear one may be used. To use such a probe, current  $I$  is fed in through any two adjacent probes and the voltage  $V$  generated across the other two is measured. The sheet resistance is then computed<sup>17</sup> from

$$R_s = \frac{V}{I} \frac{2\pi}{\ln 2} = 9.06 \frac{V}{I}$$

For very small probes, the requirement that the probe geometry be perfectly square may be difficult to achieve in practice, and the average of two independent measurements using different pairs of current probes may be utilized. Zrudsky et al.<sup>17</sup> have described a circuit which allows this to be performed automatically. The constant-current source is alternately switched from one pair of probes to the other, while a voltmeter that responds to the dc average of the two readings is simultaneously connected to the opposite pair of probes. The authors estimate that by this means a probe whose geometry deviates from a square by about 7% can be made to read to an accuracy of about 1%.

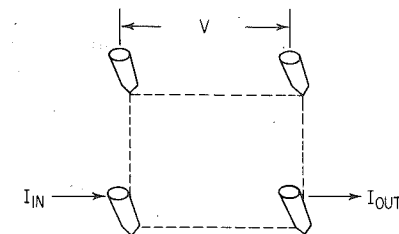


Fig. 7 Square-probe array.

### c. Temperature Coefficient of Resistance (TCR)

$\alpha_T$ , the TCR at temperature  $T$ , is experimentally determined from the relationship

$$\alpha_T = \frac{R_1 - R_2}{R_T(T_1 - T_2)}$$

where  $T_1 > T > T_2$ , and the  $R$ 's are resistance values (i.e., the geometry of the sample need not be known). When the TCR is quoted without specifying temperature,  $T$  is generally assumed to be 20°C.

A minimum of three resistance measurements must be made in order to obtain a reliable value for  $\alpha$ , the third reading being necessary as a check to determine whether the temperature treatment (up or down) has produced any permanent change in the resistance value. Where the TCR is small, it is usually advisable to plot a series of values of  $R$  vs.  $T$  (both ascending and descending). As in all resistance determinations, four terminal measurements should be used whenever possible.

To ensure accurate knowledge of the temperature at which the resistance is measured, immersion of samples in a temperature-controlled bath of a suitable nonconductive liquid (such as mineral oil) is recommended and the usual precautions such as ensuring circulation of the liquid and allowing time to come to equilibrium should be observed.

## 3. INFLUENCE OF THICKNESS ON THE RESISTIVITY OF A STRUCTURALLY PERFECT FILM

### a. Theory

As was discussed above, variations in the resistivity of a metal correspond to changes in the mean free path of the conduction electrons. Since an electron will suffer a

reflection of some sort at the surface (when it happens to reach it), the resistivity increases whenever the specimen becomes thin enough for collisions with the surface to be a significant fraction of the total number of collisions—in other words, whenever one or more dimensions of the specimen become comparable with or less than the mean free path at the temperature concerned. It should be pointed out here that collisions with the surface will be important from this point of view only if they are nonspecular, i.e., if the direction in which the electron moves after its collision is independent of its direction of motion prior to the collision. A helpful analogy is to compare the specular and nonspecular cases to the attenuation of light being propagated down light pipes having polished and diffuse surfaces, respectively.

Table 1 shows that surface scattering of electrons at room temperature becomes an important effect for most pure metals if they are less than 2 to 300 Å thick, whereas at temperatures around  $-200^{\circ}\text{C}$ , the effect is noticeable for thicknesses about one order of magnitude larger. However, the resistivity of thin films is often much higher than that of the pure bulk material, so that unless special care is taken to ensure chemically pure, imperfection-free films, the electronic mean free path will be a good deal less than the values listed in Table 1.

The possibility that the resistivity might be influenced by a reduction of one of the dimensions of a specimen was first discussed by Thomson<sup>18</sup> in 1901. A more rigorous treatment was given by Fuchs<sup>19</sup> in 1938, and almost all subsequent work in this area has been based on his approach. In particular, Sondheimer<sup>20</sup> extended the theory to include other mean-free-path effects in metals. The subject has also been reviewed, more recently, by Campbell,<sup>21</sup> and the derivation presented below includes material from all these sources.

The starting point for the analysis is the Boltzmann transport equation for electrons (for a simplified description of this, see Ref. 22)

$$-\frac{e}{m} \left( E + \frac{1}{c} v \times H \right) \text{grad}_v f + v \text{grad}_v f = -\frac{f - f_0}{\tau} \quad (6)$$

where  $f$  = nonequilibrium electronic distribution functions (for which we wish to solve this equation)

$f_0$  = electronic distribution at equilibrium

$\tau$  = relaxation time for return to equilibrium, a function only of the absolute value of  $v$ , the electron velocity

The other symbols have their usual meaning except that  $m$  will be an effective mass rather than the free-electron mass.

The  $z$  axis is taken as perpendicular to the plane of a film of thickness  $d$ , and current flows through the film in the  $x$  direction.

The use of Eq. (6) for the investigation of size effects on conductivity depends on the presence of the second term,  $v \text{grad}_v f$ , which vanishes for bulk material but not in the  $z$  direction for a thin film.

It is convenient to write

$$f = f_0 + f_1(v, z) \quad (7)$$

Substitution of (7) in (6) gives

$$\frac{eE}{mv_z} \frac{\partial f_0}{\partial v_x} = \frac{\partial f_1}{\partial z} + \frac{f_1}{\tau v_z} \quad (8)$$

since  $H = 0$  and  $E$  is in the  $x$  direction

The general solution of Eq. (8) is of the form

$$f_1(v, z) = \frac{e\tau E}{m} \frac{\partial f_0}{\partial v_x} \left[ 1 + F(v) \exp\left(\frac{-z}{\tau v_z}\right) \right] \quad (9)$$

where  $F(v)$  is an arbitrary function of  $v$  to be determined by the introduction of the appropriate boundary conditions.

To determine  $F(v)$ , we have to introduce the boundary conditions at the surfaces of the film. The simplest assumption is to suppose that every free path is terminated

by collision at the surface, so that the scattering is entirely diffuse. The distribution function of the electrons leaving each surface must then be independent of direction. Equation (9) shows that this can be satisfied only if we choose  $F(v)$  so that  $f_1(v, 0) = 0$  for all  $v$  having  $v_z > 0$  (that is, for electrons moving away from the surface  $z = 0$ ), and  $f_1(v, d) = 0$  for all  $v$  having  $v_z < 0$ .

There are therefore two distribution functions:  $f_1^+$  for electrons with  $v_z > 0$ , and  $f_1^-$  for electrons with  $v_z < 0$ . In other words,

$$f_1^+(v, z) = \frac{e\tau E}{m} \frac{\partial f_0}{\partial v_x} \left[ 1 - \exp\left(\frac{-z}{\tau v_z}\right) \right] \quad (v_z > 0)$$

$$f_1^-(v, z) = \frac{e\tau E}{m} \frac{\partial f_0}{\partial v_x} \left[ 1 - \exp\left(\frac{d-z}{\tau v_z}\right) \right] \quad (v_z < 0)$$

The solution to (8) can then be used to calculate  $J(z)$ , the current density across the film from

$$J = 2e \left(\frac{m}{h}\right)^3 \int v f dv$$

Evaluation of the above integral is facilitated by resorting to polar coordinates. Thus, we substitute  $v_z = v \cos \theta$ , and the resulting expression for  $J$  is then

$$J(z) = \frac{4\pi e^2 m^2 \tau v^{-3}}{h^3} E \int_0^{\frac{\pi}{2}} \sin^3 \theta \left[ 1 - \exp\left(\frac{-d}{2\lambda \cos \theta}\right) \cosh\left(\frac{d-2z}{2\lambda \cos \theta}\right) \right] d\theta$$

where  $\lambda = \tau \bar{v}$  is the mean free path of the electrons.

By averaging the current density over all values of  $z$  from 0 to  $d$ , an expression can now be derived for  $\sigma$ , the film conductivity:

$$\sigma = \sigma_0 \left[ 1 - \frac{3}{2k} \int_1^{\infty} \left(\frac{1}{t^3} - \frac{1}{t^5}\right) (1 - e^{-kt}) dt \right] \quad (10)$$

where  $t = \frac{1}{\cos \theta}$

$$k = \frac{d}{\lambda} = \frac{\text{film thickness}}{\text{mean free path}}$$

$\sigma_0$  = bulk-conductivity value

Approximations can be made to (10) for large and small  $k$ :

$$\frac{\sigma}{\sigma_0} = 1 - \frac{3}{8k} \quad (k \gg 1) \quad (11)$$

$$\frac{\sigma}{\sigma_0} = \frac{3k}{4} \left( \ln \frac{1}{k} + 0.423 \right) \quad (k \ll 1) \quad (12)$$

In determining  $F(v)$  in (9), it is more general (though somewhat artificial) to allow some fraction  $p$  of the electrons to be elastically scattered ( $v_x$  is the same before and after a collision) while the remainder are diffusely scattered, as before.

Equations (11) and (12) now become

$$\frac{\sigma}{\sigma_0} = 1 - \frac{3(1-p)}{8k} \quad (k \gg 1) \quad (13)$$

$$\frac{\sigma}{\sigma_0} = \frac{3k}{4} (1+2p) \left( \ln \frac{1}{k} + 0.423 \right) \quad (k, p \ll 1) \quad (14)$$

*Effect of Thickness on  $\alpha$ .* Similar reasoning may also be applied to determine the

effect of film thickness on the temperature coefficient of resistance. The result that one obtains is

$$\frac{\alpha}{\alpha_0} = 1 - \frac{3(1-p)}{8k} \quad (k \gg 1)$$

$$\frac{\alpha}{\alpha_0} = \frac{1}{\ln(1/k) + 0.423} \quad (k \ll 1)$$

In Figs. 8 and 9, curves computed by Campbell<sup>21</sup> for  $\rho/\rho_0$  and  $\alpha/\alpha_0$  as function of  $k$  are shown.

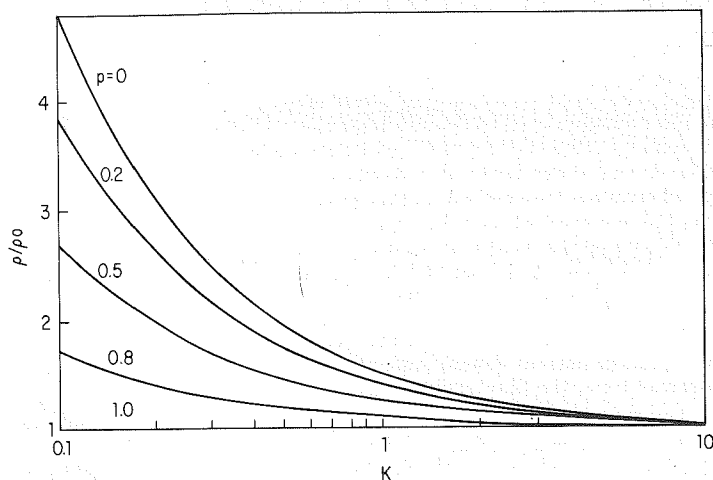


Fig. 8 Effect of film thickness on resistivity.

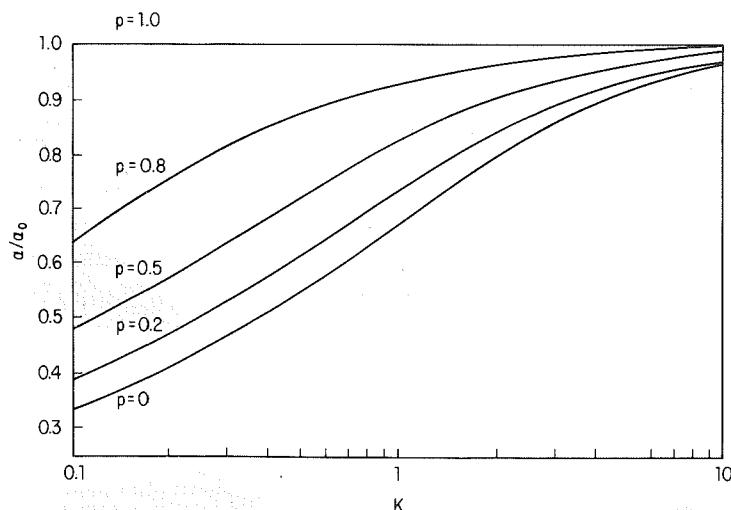


Fig. 9 Effect of film thickness on temperature coefficient of resistance.

## b. Experimental Results

The experimental verification of the formulas derived in the preceding section is not as straightforward as might be expected. This is so because of uncertainties in the exact values of the mean free path, the film thickness, and particularly the scattering factor  $p$ . In addition, the resistivity for very thin films is not always known. Finally, there are formidable difficulties in preparing sufficiently clean films to make meaningful experiments.

A detailed review of work prior to 1959 has been given by Mayer,<sup>23</sup> in whose own work films were studied under conditions which gave  $p = 0$ . Continuous measurements of resistivity and thickness were made while the film grew. The work was performed in ultrahigh vacuum with alkali metals which had previously been purified by several distillations. The films were deposited at very low deposition rates onto substrates maintained at temperatures in the order of 90°K. The surface mobility of the depositing atoms was thus extremely low, and the resulting film was therefore rough on an atomic scale, making it possible to realize the condition  $p = 0$ . At any time during the deposition, the thickness (mass equivalent) was measured using the Langmuir-Taylor ionization method.<sup>24</sup> Films were found to be continuous when their thickness exceeded three to four atomic layers (verified by observing the ohmic behavior of the films). Because of the low temperature of the measurement,  $k$  was very much less than 1 for the films investigated. Good agreement between theory and experiment was obtained for a number of alkali-metal films in the range  $k = 0.1$  to  $k = 0.5$ . Similar results using this approach have been reported by other workers.<sup>25</sup> By using atomic beams of known and well-controlled intensity for the deposition of the films, the thickness of the film at any given time could always be deduced without direct measurement.

Attempts to relate theory to the experimental data on the variation of the temperature coefficient of resistivity with thickness have not been as successful as for resistivity. It is possible that these difficulties exist because measurements have been made too close to the Debye temperature. However, a moderately good fit can usually be obtained by assuming a suitable value of  $p$ .

Although agreement between theory and experiment has been good for alkali-metal films, there is still considerable interest in films for which  $p \neq 0$ . For films with finite  $p$ , fitting theory to the experimental data introduces several problems. Nossek<sup>26</sup> has discussed some of the difficulties and pitfalls associated with attempts to ascertain the exact values of  $p$  and  $k$  in such experiments. He points out that, as a practical matter, a surface roughness of at least 10 Å has to be assumed for films. All measurements must therefore be done on films that are at least 10 times thicker than this, i.e., films in the order of 100 Å. This implies that for meaningful comparison between theory and experiment,  $k$  has to be greater than 0.1. As a result, it becomes necessary to know the thickness to an accuracy of about 6% in order to distinguish between  $p$  values as widely different as  $p = 0$  and  $p = 0.5$ . This is not an easy measurement to make under the conditions for which films of controlled  $p$  are being deposited. It might be thought that additional information concerning  $p$  could be obtained through supplemental data on temperature coefficient of resistance. However, this is also a problem because it has not been established yet whether or not  $p$  itself depends on temperature. Furthermore, even more accurate measurements are needed to obtain the necessary information.

Another difficulty associated with the measurement of  $p$  is that it may not be a function solely of the surface roughness but may also depend on the total film thickness. For example, it has been suggested by Parrott<sup>27</sup> that, in analogy with reflection of light, specular reflection takes place only if the angle of incidence of the electron at the film surface is smaller than some critical value. This would imply that specular scattering is a function of  $k$  and will be observed only in very thin films. In practice, this has been the case, although largely by default. Experimental evidence for the existence of this effect has been obtained by Chopra<sup>28</sup> by studying magnetoresistance effects in films. It was found that for films in which  $k$  was smaller than 0.5, partial specular reflection was observed, whereas for thick films with  $k$  greater than 0.5, the data could best be explained by assuming total diffuse scattering.

Abeles and Theye<sup>29</sup> have developed a method where, in addition to measuring resistivity as a function of thickness, the optical reflection and transmittance characteristics of the films in the infrared are measured. The method is applicable to relatively thick films ( $k > 1$ ), which is an advantage, experimentally. By means of this method a value of  $p = 0.2$  for gold films 265 Å thick was demonstrated. The mean free path was shown to be 236 Å. Another method which allows specific determination of resistivity  $p$  and mean free path is derived from the combined measurement of electrical resistance and Hall coefficient. In this method, also, thicker films ( $k > 1$ ) can be used. Cirkler<sup>30</sup> used this method for potassium films and obtained a  $p$  value of 0.5.

It has been found that films of certain metals such as Sn, Pb, Ag, and Au can have values of  $p$  very close to unity, provided they have received a suitable annealing treatment. For example, Gillham, Preston, and Williams,<sup>31</sup> working with transparent, highly conducting gold films deposited by sputtering onto bismuth oxide substrates, showed that essentially no variation of resistivity with thickness occurred (down to about 60 Å) if the films had been annealed for a few minutes at 350°C. Typical data are shown in Fig. 10. The apparent increase over bulk resistivity, even for relatively thick films, is not understood and is probably related to the relatively poor conditions under which the films were prepared.

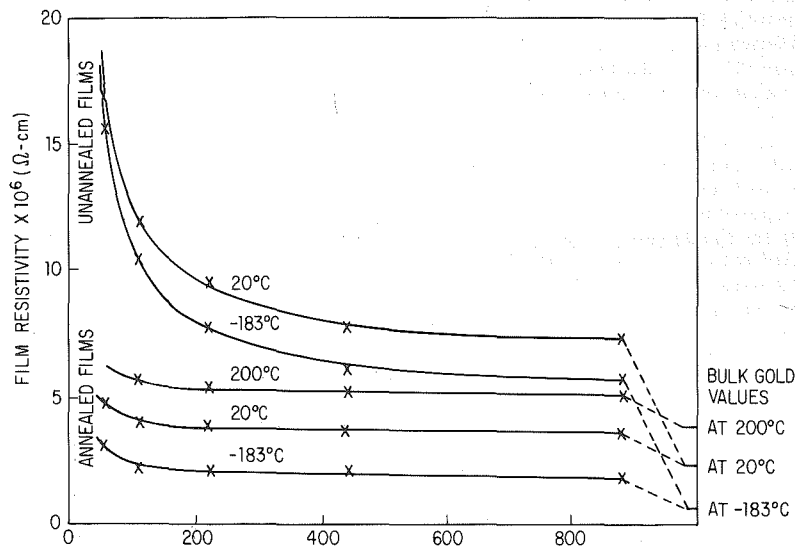


Fig. 10 Resistivity vs. thickness for gold films at several temperatures.

Similar results were obtained by Ennos<sup>32</sup> using evaporated gold films. These films, also, had close-to-bulk resistivity, down to approximately 60 Å. The temperature coefficient was investigated and found to be constant, down to about 60 Å, below which point a discontinuity appeared and the coefficient dropped off very sharply. However, the thickness-independent value was about half that of the bulk's. The reasons for this effect are not clear.

Single-crystal films of gold deposited epitaxially onto mica substrates have also been investigated.<sup>33</sup> Films with  $p = 0.8$  were obtained down to about 300 Å. By contrast, films deposited onto cold mica had  $p = 0$  even after receiving an annealing treatment of 300°C for 20 min. Annealing had a more pronounced effect on the resistivity of gold films deposited onto niobium oxide; even so,  $p$  was still found to be zero.

An interesting demonstration that the resistivity of a very thin film is influenced by the degree of specular scattering of electrons at the surface has been provided by

Lucas.<sup>34</sup> He showed that the resistivity of a "specular" film such as gold on bismuth oxide could be increased by artificially "roughening" the upper surface, i.e., converting it to a nonspecular film. The films were first made specular in the usual way by annealing for a few minutes at 350°C in air; then a small additional amount of gold (less than a monolayer) was deposited onto the specular film by either sputtering or evaporation. An increase in resistivity resulted even though additional conductive material had been added to the film. Subsequent annealing of the "roughened" film then produced the right amount of resistivity decrease, which would be expected from the additional thickness of conductive material. Lucas also found that similar results were obtained when an insulating film such as SiO was deposited over a specular gold film. This was also interpreted as due to a change in  $p$ .

Experiments related to those of Lucas have been performed by Chopra and Randlett.<sup>35</sup> The resistance of thin continuous films of gold, silver, copper, and aluminum was studied as a function of superimposed thin layers. It was found that SiO or Permalloy overlayers increased the resistance of gold films, whereas the same materials had little effect on silver. On the other hand, an overlay of germanium increased the resistance of silver films—but had negligible effect on aluminum. These and similar results suggest that an additional "roughening" of the surface does not necessarily lead to an increase in resistance. The explanation which Chopra and Randlett suggest for this is that the additional material behaves in a manner similar to that seen for adsorbed gases on the surface of films,<sup>36,37</sup> where the bonds that form may act as either donors or acceptors. Similarly, the metal overlayers are believed to modify the surface potential for the conduction electrons at the interface, influencing both their number and their mobility near the surface. Depending on the nature of the change at the interface, either an increase or a decrease in resistance may result.

Something of a special case is bismuth. This metal has an unusually large electron mean free path of between 1 and 2  $\mu$ , even at room temperature. Consequently, the effect of thickness on electron scattering can readily be observed for relatively thick films at room temperature.<sup>38</sup> An interesting consequence of this phenomenon is that electron scattering at the grain boundaries now becomes an important source of electrical resistance, since some of the grain boundaries behave like free surfaces. As a result, distinct differences occur in the resistivity of bismuth films, depending on their temperature of condensation.

Similar effects were seen by Drumheller,<sup>39</sup> who obtained data on the infrared reflection characteristics of bismuth films and correlated these with their electrical behavior. This represents one of the rare cases where grain-boundary scattering is very significant. According to Drumheller, the grain boundaries in his films fell into two distinct categories, depending on whether they divided crystallites with similar or unrelated orientations. About half the grain boundaries had a mean shunting resistance approximately equal to half the dc resistance, whereas the other grain boundaries had no appreciable effect. The major portion of the electrical resistance parallel to the film surface was contributed by grain boundaries.

Measurements on very thin metal foils rather than on deposited films have also been used to check the Fuchs theory. Such an approach was used by Andrews,<sup>40</sup> who rolled foils of extremely pure tin to a variety of thicknesses (the thinnest being 3  $\mu$ ) and measured their resistivities at very low temperature (3 to 20°K). Good agreement with theory was found for a value of  $p = 0$ .

#### 4. HALL EFFECT AND MAGNETORESISTANCE IN THIN FILMS

When a magnetic field is applied to a conductor at right angles to the direction of current flow, a voltage is developed in a plane at right angles to both the current and the magnetic field. The Hall coefficient  $R_H$  is then defined by

$$R_H = \frac{\Delta v}{Hj \Delta x}$$

where  $\Delta x$  is the width of the specimen in the plane of the Hall voltage. The significance of this coefficient stems from the fact that  $R_H = 1/Nq$ , where  $N$  is the number



of charge carriers per unit volume. Thus, since  $\sigma = Nq\mu$  (where  $\mu$  is the mobility) we have  $\mu = \sigma R_H$ , mobility measured in this manner being termed, appropriately, the Hall mobility.

In the previous section it was seen that  $\sigma$  may be reduced when the electron mean free path  $\lambda$  becomes comparable with or greater than the film thickness. The parameter  $k = d/\lambda$  was used. When a magnetic field is applied, an additional parameter  $\beta$  is needed; it is defined by  $\beta = d/r$  where  $r = m\bar{v}c/qH$  is the radius of the circular orbit of an electron in a magnetic field  $H$  and  $m\bar{v}$  is the mean momentum of an electron. Thus  $\beta \propto H$ .

The problem of the effect of a magnetic field on the resistance of a thin film was first treated in detail by Sondheimer.<sup>41</sup> His analysis predicts that with increasing magnetic field normal to the plane of the film, the resistivity will oscillate about a mean value that is greater than bulk. As for the zero field case, the increase over the bulk resistivity becomes larger the smaller the value of  $k$ . For a given field, the increase over bulk is greatest when the specular reflection coefficient  $p$  equals 0. Conductivity equals the bulk value when  $p = 1$ . Some results are illustrated in Fig. 11.

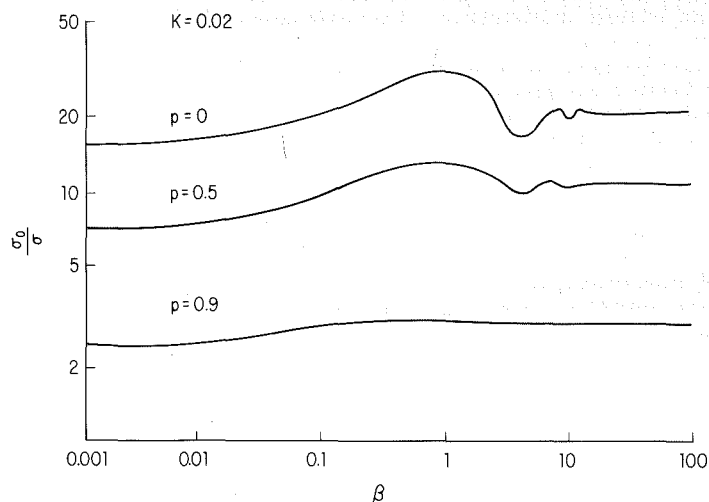


Fig. 11 Effect of magnetic field on the conductivity of a thin film.

For the Hall coefficient, the Sondheimer theory also predicts an increase over the bulk value  $R_H$ . For low fields this is given by

$$\frac{R_F}{R_H} = \frac{4}{3k} \frac{1-p}{1+p} \frac{1}{[\ln(1/k)]^2} \quad (k \ll 1)$$

where  $R_F$  is the Hall coefficient of the film. As the field is increased,  $R_F$  decreases and returns to the bulk value at  $\beta = 1$ .

Experimental attempts to verify these predictions have not always met with as much success as for the pure conductivity effects ( $H = 0$ ). This is not surprising in view of the fact that departures from bulk are greatest for weak fields where accurate measurements are most difficult to make. Jeppesen,<sup>42</sup> for example, measured a Hall coefficient 30% greater than bulk for gold films on glass but found no appreciable variation in its value over the thickness range 30 to 2,000 Å—even though a decrease in Hall mobility was seen. Cirkler<sup>30</sup> obtained the bulk value for potassium films down to 450 Å and saw only a small increase in  $R_F$  below this value (all the way down to 50 Å). On the other hand, Forsvoll and Holwech<sup>43,44</sup> found good agreement

with the Sondheimer theory for aluminum, for both the magnetoresistance and the Hall coefficient. Fair agreement with theory for Hall coefficients was also obtained by Chopra and Bahl<sup>45</sup> for gold, silver, and copper films, both epitaxial and polycrystalline. For the epitaxial films, the data indicated  $p \approx 1$ , whereas the polycrystalline films gave the best fit to Sondheimer's theory for  $p = 0$ .

In all the above, it was assumed that the magnetic field was applied normal to the plane of the film. It is, however, possible to apply the field in the plane of the film (but perpendicular to the current) thus generating a Hall voltage across the thin dimension of the film. This case has been theoretically analyzed by MacDonald and Sarginson,<sup>46</sup> who predicted that the Hall field would be less than the bulk at low magnetic fields, approaching bulk at high fields. General agreement with this prediction was obtained by Holwech<sup>47</sup> for ultrapure aluminum foils measured at temperatures of a few °K.

## 5. NEGATIVE TEMPERATURE COEFFICIENTS OF RESISTANCE IN FILMS

### a. Discontinuous Films

In the preceding sections it was assumed that the films were completely continuous and that the film thickness was uniform everywhere. However, as is discussed in Chap. 8, thin films are anything but continuous during their early stages of growth. Instead, they are made up of small islands which may or may not be physically connected to one another. Even if the individual islands possess resistivities approaching the bulk and are multiply interconnected, a high resistivity will still be measured—for purely geometrical reasons—but the temperature coefficient of the film should be close to the bulk value. In practice, however, the temperature coefficient of very thin but moderately conductive films rarely approaches the bulk value; in fact, it is rarely even positive. Instead, such films usually exhibit large negative temperature coefficients, and it is with films of this type that we are concerned in this section. Electrical conduction in films of this type has been reviewed by Neugebauer and Wilson,<sup>48</sup> and the following two sections contain a good deal of material from their article.

Extensive measurements on the electrical properties of thin discontinuous films have been made by Mostovetch and Vodar.<sup>49</sup> Film resistivity, temperature coefficient of resistance, and field dependence of resistances were investigated. The resistance vs. temperature curves obtained by them for discontinuous films of three metals are shown in Fig. 12. Good fits were obtained using equations of the type

$$R = A_0 T^{-\phi} e^{\theta/kT} \quad (15)$$

where  $A_0$ ,  $\phi$ , and  $\theta$  are constants of the particular film. The films were generally nonohmic, their resistance decreasing with applied field. A linear dependence of resistance on the square root of the applied field was found for sufficiently high applied fields.

Work published by Minn<sup>50</sup> has clearly indicated (Fig. 13) the rapidly decreasing temperature coefficient of resistance with increasing film resistivity (decreasing film thickness).

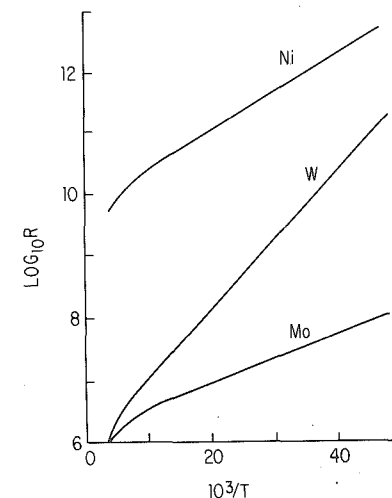


Fig. 12 Resistance vs. temperature for discontinuous films of three different metals.



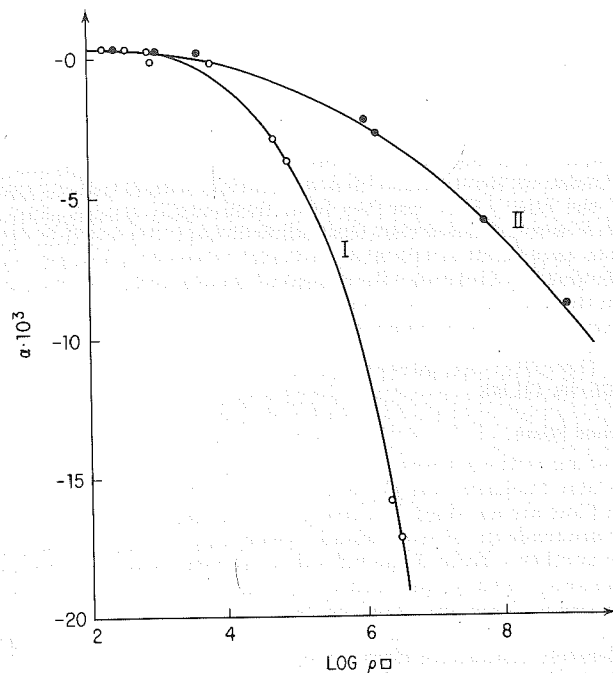


Fig. 13 Effect of sheet resistance on temperature coefficient of resistance.

In the experiments of Neugebauer and Webb,<sup>51</sup> nickel, platinum, or gold was evaporated onto Pyrex glass substrates to give films of average thickness ranging from a few to several tens of angstroms. The resistance of a freshly deposited film always increased with time after the deposition. This was due partly to the decreasing film temperature, which was most likely higher during deposition than the nominal substrate temperature—and partly to some annealing which occurs in films even at room temperature. The film resistance usually stabilized after aging for a few hours, and the measurements were undertaken only with films which were completely stable in the time and temperature interval of the measurements.

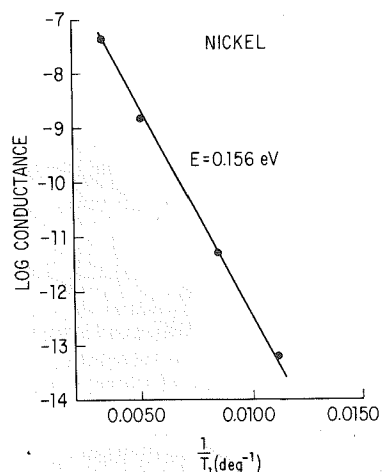


Fig. 14 Typical curve of conductance vs. temperature for a discontinuous nickel film.

Figure 14 is a typical curve showing the dependence of conductance on temperature for a nickel film a few angstroms thick. Good linearity of the log plot of conductance vs.  $1/T$  exists. The temperature interval was from 77 to 373°K. Because of the high activation energy for conduction in this particular film, it was possible to vary the conductance over six orders of magnitude within a temperature interval of about 200°K.

Many of the films prepared by Neugebauer and Webb obeyed Ohm's law very well, and the conductivity was found to be essentially

independent of field up to several hundred volts per centimeter. However, in some films, particularly the thicker ones, deviations from Ohm's law could be observed at quite low fields, especially at lower temperatures, and a characteristic square-root dependence of applied field was seen. At sufficiently small fields, however, the conductivity always became independent of field, even in these (thicker) films.

Figure 15 shows the log plot of conductance vs.  $1/T$  for six platinum films of progressively greater thickness. A film in this series was made thicker by successively evaporating more platinum onto the previous film under otherwise identical conditions. The thickest film was only 10 to 20 Å thick (average thickness). Increasing the average film thickness resulted in an increase in the average particle dimensions, assuming all other conditions remained the same.

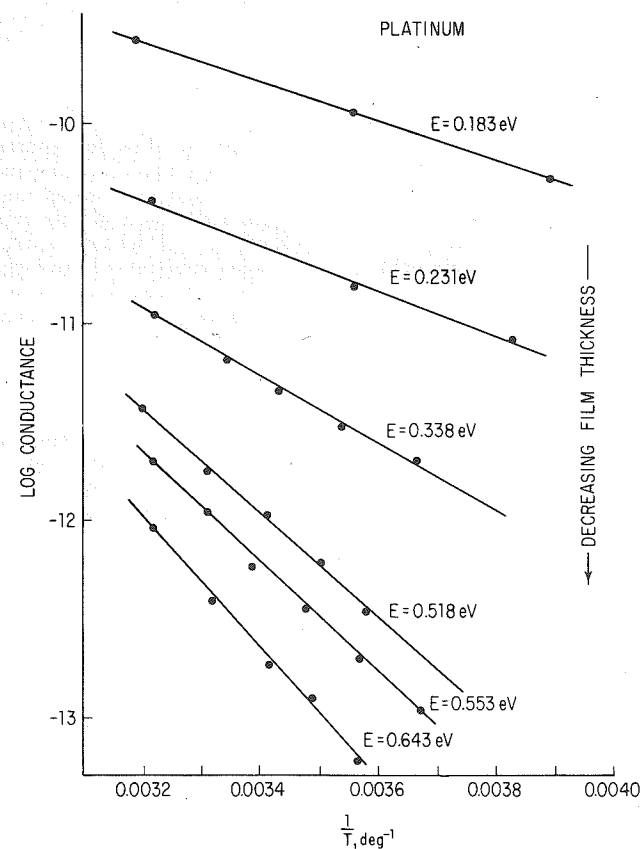


Fig. 15 Conductance vs. temperature curves for platinum films of varying thickness.

Hill<sup>52</sup> has investigated the electrical behavior of discontinuous gold films evaporated onto soda glass or borosilicate substrates. In his configuration, another electrode (to which a dc bias voltage could be applied) was deposited on the back side of the substrate so that the film to be measured was made part of a capacitor structure. The discontinuous metal films measured by Hill were relatively conductive ( $R \approx 5 \cdot 10^3$  ohms) and consisted of rather large islands (260 Å) with large average spacings ( $\sim 50$  Å). Variations of the resistance of the film with bias voltage were found for both types of glass substrate. The results are shown in Fig. 16.

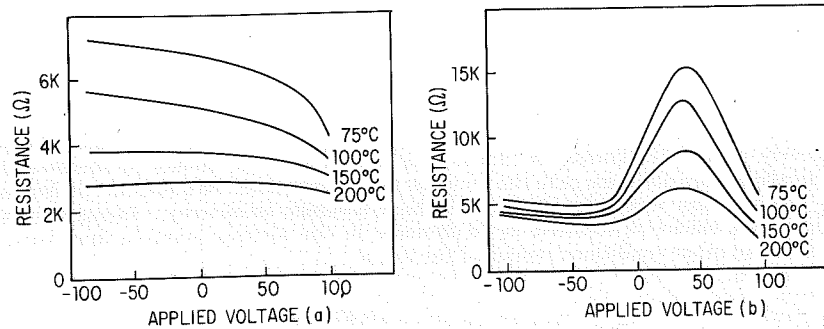


Fig. 16 Resistance of discontinuous films as a function of bias applied to an electrode on the back side of the substrate. (a) Soda glass. (b) Borosilicate glass.

Negative temperature coefficients can also occur in films for another reason. Thus, it might be expected that when the substrate has a high thermal expansion and the film a low one, the distance between particles might increase as the substrate expands relative to the films. An example where a situation of this type prevails is gold on Teflon. This has been discussed by Neugebauer,<sup>53</sup> who gives data showing, for example, that relatively thin gold films on Teflon substrates have large negative temperature coefficients in the order of  $-0.017/^{\circ}\text{C}$ . As the films are increased in thickness, the temperature coefficient becomes progressively more positive, having a value for the thickest films of the order of  $0.0012/^{\circ}\text{C}$ .

#### b. Theories of Conduction in Discontinuous Films

**(1) Transport by Thermionic Emission** Historically, this was the first mechanism postulated to explain current transport between islands. Because of the experimental temperature dependence of the thermionic current, functional agreement is obtained with experiment. However, since the activation energies observed in discontinuous film conduction are very much smaller than the work functions of the corresponding bulk metals, it has been necessary to postulate (1) that this lower activation barrier is due to an overlap of the image-force potentials of two islands very close to each other; (2) that a small particle has a lower work function than bulk material; or (3) that the shape of a small particle brings with it a reduced work function. However, if electrons are injected into the substrate,<sup>54</sup> it is necessary to consider only the difference between the metal work function and the electron affinity of the insulator.

In the treatment of Minn,<sup>50</sup> for instance, the barrier between particles is taken to be lower than the work function of the bulk material by an amount  $\gamma q^2/d$  due to image forces, where  $\gamma$  is a function of the size of the islands and the distance  $d$  between them. The final expression for the conductivity is

$$\sigma = \frac{BqTd}{k} \exp - \left( \frac{\phi - \gamma q^2/d}{kT} \right)$$

where  $B$  is a constant (characteristic of each film) and  $\phi$  is the work function for the bulk material.

A remarkably good fit to experimental values of the conductance vs. the square root of the applied potential for thin gold films at various temperatures has been obtained by Skofronick et al.<sup>55</sup> using a thermionic model. From this fit, the average distance between islands was deduced, and found to be quite large—as much as 59 Å in one example. On the other hand, the barrier height to be surmounted by the thermal electrons turned out to be very small, ranging from 0.0074 to 0.0258 eV for zero applied voltage in their examples.

**(2) Transport by Activated-charge-carrier Creation and Tunneling** This mechanism has been proposed by Neugebauer and Webb<sup>51</sup> for the limit of very small islands of

uniform size. For such a case they have postulated that the activation energy is that required to transfer charge from one initially neutral island to another some distance removed. The importance of this electrostatic energy in electrical conduction between small particles has been indicated by Gorter<sup>56</sup> and Darmais.<sup>57</sup> This energy will be of the order of magnitude  $q^2/r$ , where  $q$  is the electronic charge and  $r$  is the average linear dimension of the particles. Only electrons or holes excited to states of at least this energy above the Fermi level will be able to tunnel from one neutral island to another. The process is thus an activated one leading to an equilibrium number of charged islands.

Note that the transfer of charge from a charged island to a neutral one is not activated, because it does not lead to a net increase of the energy of the system, in contrast to the case for two initially neutral particles. Interactions between charges are neglected, leading to the requirement that  $n \ll N$ , where  $n$  is the number of charges and  $N$  is the number of particles. This requirement is best met when the islands are very small.

It should also be noted that tunneling from island to island is different from tunneling between two electrodes kept at fixed potentials by a battery, since the Fermi levels of the particles are not held fixed. When an electron tunnels between two electrodes whose Fermi levels are fixed, no electrostatic work has to be done since the positive charge left behind is immediately neutralized and no energy is added to the system. When, however, an electron is removed from one island and is added to another some distance removed, energy is added to the system.

In Neugebauer and Webb's model, a "film" consists of a planar array of many small, discrete metal islands of linear dimension  $r$ , separated by an average distance  $d$ , which is also small. At equilibrium, and at any temperature above  $0^{\circ}\text{K}$ , a certain number of particles are charged, having lost or gained an electron to or from initially neutral particles some distance away. If the activation energy is supplied by thermal means, the equilibrium number of charge carriers will then be of the order of

$$n = Ne^{-\epsilon/kT}$$

where  $\epsilon$  is the effective activation energy, which approximately equals  $q^2/r$ .

Thus, the model pictures a large number of metal islands  $N$  of which a relatively small number  $n$  are charged. The equilibrium concentration of these charge carriers is maintained thermally, and there is only random motion of the charge in the absence of a field. Applying a field displaces the relative position of the Fermi levels of neighboring particles, and the tunneling probability increases for a transition of charge from island to island in the field direction, and decreases a corresponding amount against the field direction.

The final expression derived for the conductivity is

$$\sigma = \frac{A \sqrt{2m\phi}}{h^2 D} \exp \left( \frac{-4\pi d}{h} \sqrt{2m\phi} \right) B \exp \left( \frac{-q^2/Kr}{kT} \right) \quad (16)$$

where  $A$  and  $B$  are constants,  $\phi$  is the potential barrier between islands,  $m$  is the electronic mass, and  $K$  is a dielectric constant.

This equation predicts that the conductivity of a film consisting of discrete islands varies exponentially with temperature and is independent of applied field.

**(3) Transport by Tunneling between Allowed States** In this treatment by Hartman,<sup>58</sup> use is made of the quantization of the energy levels in a small particle. It is postulated that in order for charge transfer to occur between two islands by tunneling, the two energy levels between which the electron tunnels must be "crossed," i.e., their energy widths must overlap. Such an overlap is most likely if the width of the energy levels is great. The width of an energy level in a particle is assumed to be determined by the lifetime of an electron in that level, which, in turn, is assumed to depend on its tunneling probability out of this level. The width of the  $n$ th level is, from the uncertainty principle,

$$\delta E_n \approx \frac{\hbar^2}{a} \left( \frac{2E_n}{m} \right)^{\frac{1}{2}} P(E_n)$$

where  $a$  = linear dimension of a one-dimensional box,  $E_n$  = energy of  $n$ th level, and  $m$  = electronic mass.

Also,  $P(E_n)$  is the probability of tunneling out of level  $E_n$  and is given by

$$\exp\left(-\frac{2}{\hbar} \int_{x_1}^{x_2} \{2m[V(x) - E_n]\}^{1/2} dx\right)$$

where  $V(x)$  is the barrier height at a distance  $x$  between islands, and  $x_1$  and  $x_2$  are the values of  $x$  where  $E_n = V_x$ .

Since the tunneling probability is small from levels of energy which are low compared with the barrier height, the width of this level is small, and overlap with a corresponding level in the second island is unlikely. Tunneling could therefore not occur. However, if the electron is activated into a higher level (from which the tunneling probability is larger and, therefore, the level is wide), overlap of the levels of the two islands is much more probable. The energy required to activate an electron from the Fermi level to the first excited level is taken as the activation energy for conduction in this model.

The final equation for the conductivity becomes

$$\sigma = \sigma_0 \exp\left(\frac{-\Delta E_n}{kT}\right) \quad (17)$$

where  $\sigma_0$  is proportional to  $P(E_n + 1)$  and

$$\Delta E_n = E_{n+1} - E_n$$

**(4) Transport by Substrate-assisted Tunneling** In this model (proposed by Hill<sup>52</sup>), the dielectric substrate is assumed to have a large number of trapping sites between the conduction and valence bands, and the electrons tunnel into these traps rather than make the jump from island to island all at once. The activation energy for conduction in this model is taken to be the energy required to activate an electron from one trap to the trap of the next highest energy in the substrate (Fig. 17). This

energy will depend on the distribution of traps in the band gap. Since the process occurs by several steps, the tunneling probability is very much higher than for tunneling in one step, because of the strong  $e^{-d}$  dependence.

In the example shown, if there is no trap at the Fermi level, tunneling must occur from island I into trap A, below the Fermi level. However, since tunneling from A into island II is not possible (because there are no empty states in II), the electron must be thermally activated to trap B (above the Fermi level), from which it can now tunnel into island II. It is clear that through this mechanism tunneling can occur over larger distances.

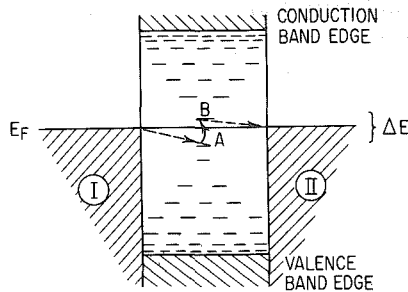


Fig. 17 Model for substrate-assisted tunneling.

By making the discontinuous film one electrode of a capacitor, with the substrate as the dielectric, and applying a dc bias (as described in Sec. 5a), the Fermi level in the substrate is lowered toward the valence band. Since the density of the traps and the separation between them depend on their position in the band gap, the activation energy for conduction will change if the position of the Fermi level is changed. In particular, Hill<sup>54</sup> assumed many traps near the band edges, very close to each other, and fewer of them (farther apart) in the middle of the gap. Hill's experimental results on the resistance with applied bias voltage, shown in Fig. 16 for two types of glass substrates, can be explained by taking the Fermi level in the glass at the appropriate position in the gap.

In later papers, Hill has developed a more general version of his theory.<sup>54</sup> In the resulting equations, the current density in the film is expressed as a direct function of the structure of the film, the electrical properties of the substrate, the applied voltage, and the temperature. According to this theory, charge is always transferred between particles by way of the substrate, either through trap hopping (discussed above) or through thermionic emission into the conduction band of the insulator that constitutes the substrate. Experimental evidence is provided to support the theory, and it is also shown that the bias effect (Fig. 16) can be observed only when the substrate contains mobile alkali ions and when the spacing between particles exceeds 30 Å.

**(5) Other Models** A modified version of Neugebauer and Webb's theory which incorporates some of the ideas discussed by Hill has been proposed by Herman and Rhodin.<sup>59</sup> They examined films of silver, gold, and platinum deposited onto single-crystal sodium chloride substrates in vacua of the order of  $10^{-7}$  to  $10^{-8}$  Torr. Their results suggested that tunneling occurred through the substrate rather than through the vacuum between the particles. The current carriers were believed to be contributed to the insulator surface regions by the metallic microparticles, and in addition, an activation energy was necessary for tunneling to occur. This energy is electrostatic in nature and is dependent upon the average size and separation of the microparticles. The presence of traps in the substrate was suggested, and a distinction was drawn between the filled traps under the metallic particles and those between the particles (traps in the two regions not necessarily being at the same level). Although themselves electrically neutral, the presence of the metallic microparticles could cause energy differences between the traps, because of image forces. The model thus appears to combine some of the features of Neugebauer and Webb and of Hill.

As might be expected, films that are partially continuous have their resistances governed by both an activation mechanism as well as the "normal" lattice-scattering mechanism. Feldman has studied films in this thickness range.<sup>60</sup> Their resistivity can be expressed by an equation of the form

$$\rho = \rho_0[1 + \alpha(T - 273)] + Ce^{\theta/kT}$$

where the first term is the normal temperature dependence and the second represents a thermally activated process of some kind. Figure 18 shows a resistance vs. temperature curve for films of this type. In the first portion of the curve, the activated conductivity contribution dominates—after which the conventional temperature coefficient becomes more important. Note that the separate grains that made up the film must have been reasonably pure, since the conventional temperature-coefficient contribution was fairly close to the bulk value.

Another model in which conduction in discontinuous films is the result of two mechanisms operating together has been suggested by Milgram and Lu.<sup>61</sup> It was shown that the  $I$ - $V$  characteristics of their films (chromium on glass overcoated with SiO) could be well described by an equation of the form

$$I = AV + BV^n$$

where  $A$  and  $B$  are constants which are temperature-dependent and  $n$  is a number which approaches 2.0 at high temperatures. At low temperatures ( $\sim 4^\circ\text{K}$ ),  $B$  is the dominant coefficient, being in the order of  $10^{-7}$ , whereas  $A$  is less than  $10^{-10}$ . However, at high temperatures (400°K),  $A$  dominates and is in the order of  $10^{-8}$ , whereas  $B$  is approximately  $10^{-8}$ . The authors believe that the linear portion is due to tun-

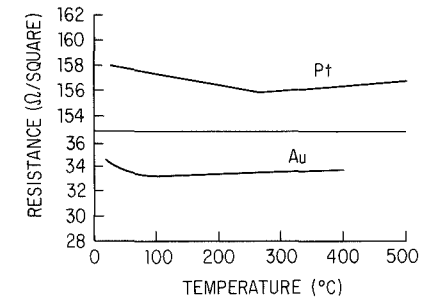


Fig. 18 Sheet resistance vs. temperature for partly continuous films.

neling via thermally activated traps by a mechanism similar to that of Hill, although  $A$  could not be fitted by a single activation energy. The  $B$  term of their equation is ascribed to space-charge-limited current, which should follow a  $V^2$  law. At high temperature and near zero field the current is carried mainly by thermally excited carriers whose number is a function of the temperature and density of trapping centers. At low temperature the conduction is dominated by the space-charge-limited current.

**(6) Range of Applicability of Various Models** It appears that the model of Neugebauer and Webb satisfies the qualitative observations on the conductivity of discontinuous films for smaller particle size, whereas Hill's mechanism offers an acceptable explanation for the larger-particle larger-gap films. Quantitative correlation of activation energies with island sizes is necessary to compare these two models further. Field-effect measurements on smaller particles should also be significant.

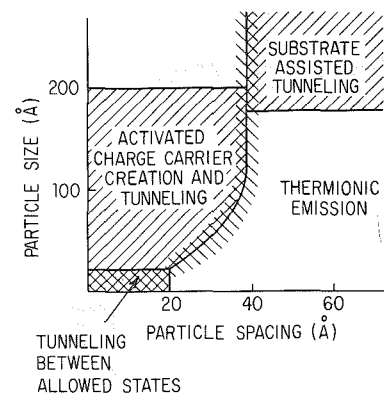


Fig. 19 Range of particle size and spacing over which various theories of conduction in discontinuous films are applicable.

temperature coefficients. Since the impurities that are trapped in a film come largely from the background gases present during evaporation, the condensing film will act as a "getter" for these gases. This phenomenon is well known and has been exploited in many areas such as, for example, the titanium sublimation pump, which has a strong affinity for virtually everything except the rare gases.

One consequence of this gettering action by freshly deposited films is that, as deposition proceeds, the residual gas background is reduced and, consequently, a purer film results. The resistivity of a film thus frequently comes closer to the bulk value as the film grows (assuming constant deposition rate) until the point is reached when the rate of gettering just equals the rate at which fresh impurities enter the vacuum chamber. Because of this, the temperature coefficient of the initial layers of the film will often be strongly negative, whereas the coefficient is just as strongly positive for the upper layers. At some point the temperature dependence of the two layers will just cancel, and this has led some workers to report a "magic thickness" at which zero temperature coefficient is obtained.

Evidence that the resistivity and temperature coefficient of tantalum films become independent of their thickness (down to at least 500 Å), if they are sufficiently pure, has been provided by Maissel and Schaible.<sup>62</sup> Using bias sputtering, a process which prevents films from doing any appreciable gettering (see Chap. 4), they showed that resistivity variations due to thickness became smaller and were eventually eliminated as the gettering ability of the films was progressively reduced. This is illustrated in Fig. 20.

Figure 19 gives the various regions of island size and separation at which the various conduction mechanisms are most applicable.

### c. Continuous Films

The negative temperature coefficients discussed above apply to films which are still in the island stage of growth and are a consequence of the energy required for electrons to cross the spaces between the islands. However, negative temperature coefficients are commonly seen in metallic films which are well past the island stage and which may be many thousands of angstroms thick.

It appears to be generally true that negative temperature coefficients are not seen in continuous metal films unless impurities are present. Also, the greater the deviation of the film resistivity from the bulk resistivity, the more negative the temperature coefficient. Thus, much work in thin film resistors (see Chap. 19) has been devoted to attempts to find high-resistivity films that do not have large negative

As noted above, the contribution of grain boundaries to the resistivity of metal films is small. However, impurities trapped in a film during its deposition can subsequently migrate to the grain boundaries where there is a high probability that precipitation will occur. In addition, it is well known that diffusion along grain boundaries is several orders of magnitude faster than it is in the bulk; so contamination from external sources may also occur on life.

The effects of grain-boundary oxidation have been studied in some detail for tantalum.<sup>63</sup> Films of this material sputtered under reasonably clean conditions and then subsequently heat-treated at 250°C showed only very small increases in resistivity when heat-treated in vacuum. On the other hand, samples heated in air showed increases of over 100%. Similar films depos-

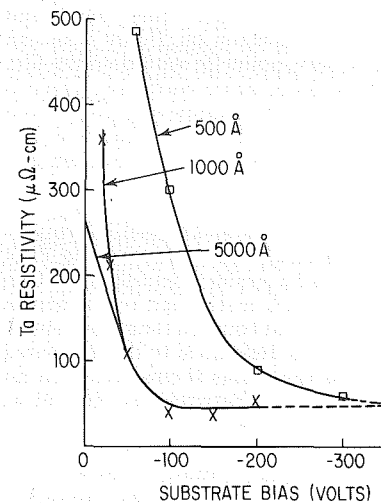


Fig. 20 Lack of dependence of resistivity on film thickness when gettering is suppressed.

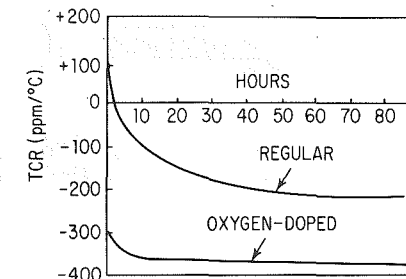


Fig. 21 Temperature coefficient of resistance of tantalum films as a function of heat treatment in air at 250°C.

ited in an atmosphere containing 0.1% of oxygen showed increases in resistance when vacuum-heated as well as when air-heated. None of the resistivity increases, even those obtained for the pure films heat-treated in air, could be explained on the basis of simple surface oxidation.<sup>64</sup> It was shown that grain-boundary oxidation of the films was occurring both internally because of migration of trapped oxygen, as well as externally, in from the surface.

Such oxidized grain boundaries give rise to negative temperature coefficients in a manner that is closely analogous to what is observed in discontinuous films. Some results, showing TCR as a function of heat treatment, are shown in Fig. 21. Thus it is clear that films which have undergone grain-boundary oxidation are not electrically continuous, even though they are physically continuous. At this time, no quantitative theory has been developed to deal with negative temperature coefficients in films of this type. This is not surprising, since the problem is complicated by the fact that the effective spacing between grains varies as a function of depth in the film.

## 6. HIGH-FREQUENCY CHARACTERISTICS OF THIN FILMS

As was discussed above, negative temperature coefficients can occur in thin films because of lack of electrical continuity between the grains. In the case of very thin (agglomerated) films, the grains are separated by air spaces, whereas in thicker films the space between the grains is filled with dielectric material. In either case, the negative temperature coefficient arises because of the activation energy associated with electron transitions from grain to grain.

A structure in which metallic grains are separated by small spaces is electrically equivalent to a series of capacitors, and consequently its ac impedance is less than the dc value. Furthermore, one would expect this difference between ac and dc conductance to become progressively larger as the temperature is reduced, since the dc resistance of discontinuous films increases rapidly with decreasing temperature.

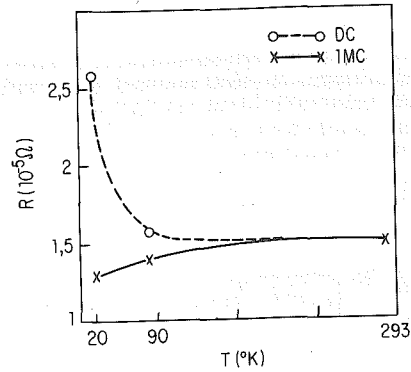


Fig. 22 Comparison of dc and high-frequency resistance of a discontinuous film as a function of temperature.

In making measurements of the high-frequency falloff in resistance of thin films, allowance must be made for a geometrical effect which has nothing to do with the microstructure of the film. This effect, which has been discussed by Howe,<sup>66,67</sup> arises because of capacitive coupling between one half of the film and the other. This can be visualized by imagining a film initially folded over upon itself as shown schematically in Fig. 23a and then opened up as shown in Fig. 23b. Although the capacitance between the adjacent portions is reduced as the film is "straightened out," it does not go to zero, and finite capacitive coupling between the two halves of the film occurs.

A curve showing the magnitude of this geometrical effect, as calculated by Howe,

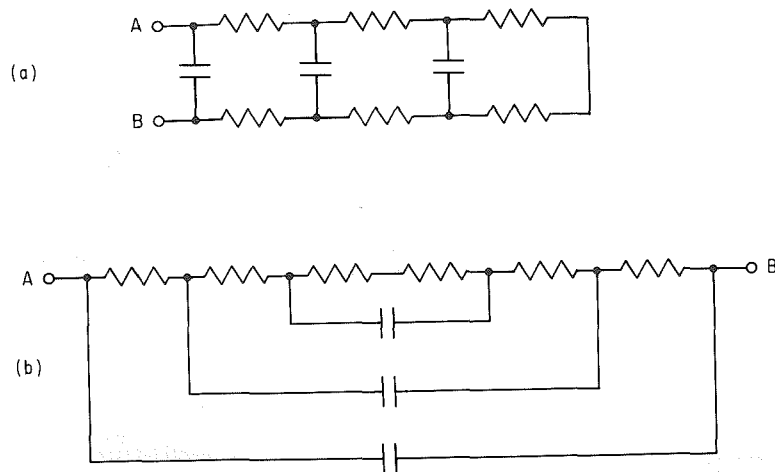


Fig. 23 Representation of capacitive coupling between the two halves of a thin film.

An excellent illustration of this may be seen in Fig. 22, taken from Offret and Vodar,<sup>65</sup> for platinum on Pyrex. As can clearly be seen, under dc conditions the film exhibits a temperature coefficient which is close to zero at room temperature but which becomes increasingly more negative as low temperatures are achieved. However, at a frequency of 1 MHz the spaces between the grains are effectively short-circuited by the alternating current, and a positive temperature coefficient is seen, reflecting the TCR of the metallic grains themselves. Note also that at sufficiently high temperatures the direct current between the grains is large enough for the resistance to be dominated by that of the grains themselves, and no difference is seen between the dc and ac values of resistance.

is shown in Fig. 24. To compute the resistance-frequency behavior of a particular sample of dc resistance  $R$  at frequency  $f$ , it is necessary to know the capacitance per unit length  $c$ . This is a number of the order of 0.1 to 1 pF cm<sup>-1</sup>, depending on the aspect ratio of the resistor. For example, a resistor of 20 squares has a value of 0.12 pF cm<sup>-1</sup> while a resistor of 10 squares has a value of 0.17 pF cm<sup>-1</sup> (dielectric constant of substrate = 1).

Thus, unless the effect of the distributed capacitance is known, no quantitative interpretation can be made of the falloff with high frequencies. For example, Fig. 25<sup>68</sup> shows the frequency-resistance behavior of a lead sulfide film at 25°C where it is seen that at low frequencies the distributed capacity effect dominates, while the intercryst-

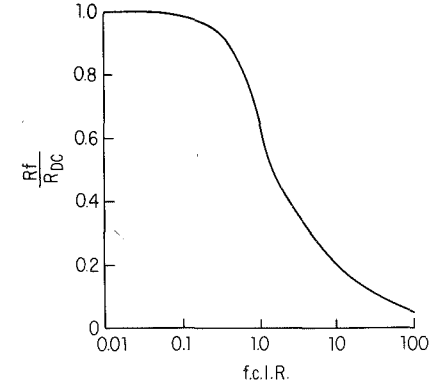


Fig. 24 Falloff in the resistance of a thin film with increasing frequency as a consequence of capacitive coupling.

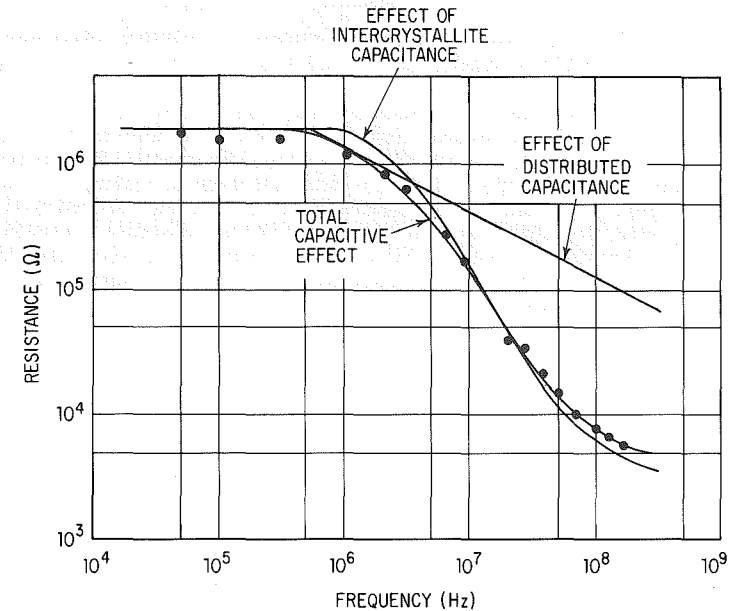


Fig. 25 Resistance vs. frequency behavior of a PbS film, showing both geometrical and structural contributions.

allite capacitance is the prime factor at high frequencies.

One way to avoid the distributed capacitance effect and thus see only the frequency falloff due to structure is to fabricate the film in the form of an annulus as shown in Fig. 26. This configuration is then made to terminate one end of a transmission line, the strength of the signal reflected off the end being a measure of the ratio in impedance between the sample and the line. The other end of the line is terminated by a short circuit so that capacitance effects are balanced out and only the resistive component is measured.

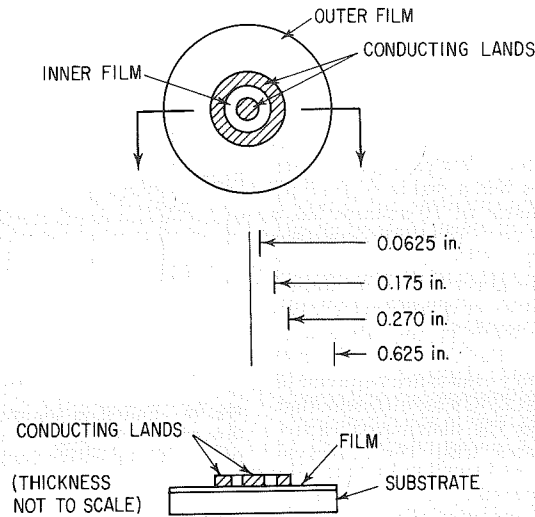


Fig. 26 Annular geometry used for studying resistance vs. frequency characteristics of thin films.

Using measurements of this type, Maissel<sup>63</sup> was able to show that tantalum films of high purity and having a positive temperature coefficient exhibited no resistance falloff to frequencies as high as 10 kHz. On the other hand, films which had developed large negative temperature coefficients as a result of heating in air showed a pronounced resistance falloff at frequencies in excess of a few hundred MHz. As might be expected, at sufficiently high frequencies the ac resistance approached the dc resistance which the film had exhibited prior to being aged, confirming the fact that heat treatment causes grain-boundary oxidation from the surface of the film down toward the substrate.

## 7. INFLUENCE OF HEAT TREATMENT

### a. Annealing

As we have seen, unless a great deal of special care is taken during their deposition, films will, in general, contain a host of structural defects. In view of the fact that these represent a considerable departure from equilibrium, we would expect some, if not all, of these defects to anneal out of the film on the application of relatively mild heat treatment. This should lead to a corresponding decrease in film resistivity, and in general this is the case. In certain instances, however, heat treatment may lead to an increase in resistivity because of the effects of oxidation and/or agglomeration.

General theories of annealing as well as methods for the analysis of annealing curves are discussed by Damask and Dienes.<sup>6</sup> Of more interest for films are the kinetics of processes distributed in activation energy. These have been reviewed in some detail by Primak.<sup>69</sup> A theory of resistivity changes associated with the annealing of defects specifically aimed for films has been presented by Vand.<sup>70</sup> This will now be discussed in more detail.

Vand begins by postulating that the distortions whose decay is observed during annealing are what he calls the "combined type," that is, vacancies and interstitials in close proximity to one another. These require a characteristic energy  $E$  to make them combine with and cancel one another, but the energy required to bring about their migration toward each other is considered to be negligible.  $E$  can vary from zero all the way to the activation energy for self-diffusion.

If  $r(E)$  is the contribution to the residual resistivity made by one distortion per unit volume, and  $N(E) \Delta E$  is the number of distortions per unit volume that have decay energies between  $E$  and  $E + \Delta E$ , then the total contribution to the resistivity made by imperfections is given by

$$\rho_i = \int_{-\infty}^{\infty} r(E)N(E) dE$$

The value of  $\rho_i$  may change with time as a result of annealing. A distribution function describing the "energy spectrum" of the distortions in the film can then be defined. It will be of the form  $F_0(E) = r(E)N(E)$ .

As a result of his analysis, Vand shows that

$$F_0(E) = -\frac{1}{kU} \frac{d\rho}{dT} \quad (18)$$

where  $d\rho/dT$  is the slope of the resistance vs. temperature curve obtained when the film is allowed to heat up at a uniform rate, and its resistance is measured as function of temperature (and, therefore, also of time). Allowance is made for the portion of  $d\rho/dT$  that is due to the normal temperature coefficient of resistance.  $k$  is Boltzmann's constant and  $U$  is defined by

$$U = \frac{u(u+2)}{u+1} \quad (19)$$

where

$$u + \log u = \log 4nt\nu_{\max} \quad (20)$$

$n$  = number of atoms that can initiate a defect (this number is not known, exactly, but is estimated as being close to 10)

$\nu_{\max}$  = Debye cutoff frequency for the lattice

$t$  = time that it took to reach the particular temperature at which  $d\rho/dT$  was measured

$u$  is readily obtained by successive approximation in Eq. (20) so that  $F_0(E)$  may be plotted against  $E (= u k T)$  to give the "lattice-distortion" spectrum.

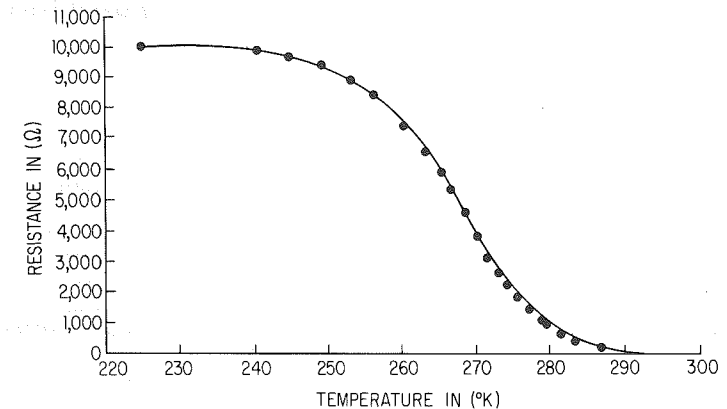


Fig. 27 Annealing curve for an evaporated gold film.

An example of a curve of resistance vs. temperature and time for an evaporated gold film<sup>71</sup> is shown in Fig. 27.

To obtain the distribution function  $F_0(E)$ , it is now necessary to measure the slope of this curve at successive values of temperature (and, hence, time), correct the resistivities for temperature coefficient, and substitute the results in Eq. (18). In

Eq. (20) the value of  $u$  can be calculated for any given values of  $t$  [hence  $U$  in Eq. (19) is obtained]. The results of this analysis for the curve of Fig. 27 are shown in Fig. 28 for two different deposition rates. The results show that for lower deposition rates, fewer defects are formed, and that these have a smaller decay energy. Separate experiments showed that  $E_{\max}$  and  $F_{0\max}$  were independent of film thickness over a range of 100 to 900 Å, for constant deposition rate.

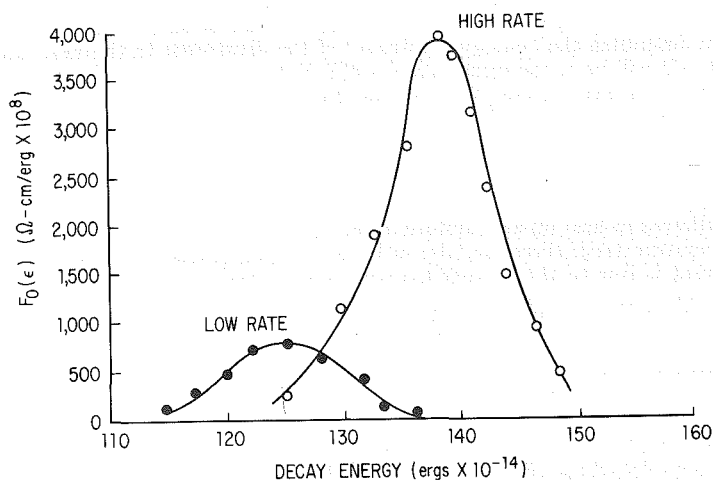


Fig. 28 Lattice-distortion spectrum of gold films deposited at high and low rates.

In a later study, Wilkinson<sup>72</sup> also investigated the effect on the defect spectrum of various background pressures of nitrogen, ranging from  $10^{-7}$  to 0.11 Torr. Three groups of distortions were found at approximately 80, 100, and 120 ( $\times 10^{-14}$  erg), the exact values depending on the conditions of preparation. It was shown that the number of distortions decreased as the nitrogen pressure increased, particularly for the two defect types of lower energy. It was argued that the effect of the nitrogen could not be to assist the gold atoms (via collision) to find their correct lattice positions, since the average kinetic energy of nitrogen molecules at 300°K is only 5 to 10% of the distortion decay energy. However, since a distortion is estimated to contain approximately 10 atoms, it is conceivable that during the growth of the film, the nitrogen atoms act separately on the individual atoms that compose the distortion, thus allowing it to be destroyed.

An analysis of defect distribution by Vand's technique has been performed for carbon films by Troyoda and Nagashima.<sup>73</sup> They found the values of the peak energies to be thickness-dependent. Specifically, for films 110 Å thick the peak was at 2.3 eV; for 380-Å-thick films the peak was at 1.6 eV; whereas for 2,000-Å films it was 1.4 eV. Films had to be annealed to about 900°C before a resistivity close to the bulk value could be achieved.

An alternative explanation suggested to account for the decay of resistance on annealing is that vacancies which are present in the film in numbers that far exceed their equilibrium value coalesce into progressively larger groups until they finally organize into sheets and collapse to form dislocation rings.<sup>74</sup> Supporting evidence for this hypothesis was obtained from indirect measurement of the volume change that occurred in evaporated nickel films when they were annealed. This volume change (deduced from observations on strain) was found to correspond fairly closely with the resistivity changes. Initially the film expands because of coalescence of vacancies and then, at higher temperatures, it contracts because of the collapse into dislocation rings.

It was observed earlier that some metals have lower electrical resistivity in the

liquid state than in the solid. If the amorphous state can be regarded as closely analogous to a supercooled liquid, we would expect such films to have their lowest resistance while in the amorphous state, and annealing should then lead to an increase rather than a decrease in their resistance. Such behavior has, in fact, been observed in a number of metals. For example, bismuth films<sup>75</sup> deposited at 2°K reached a maximum in resistivity at approximately 80°K as the temperature was slowly raised to 300°K. Thereafter, the resistivity decreased with further heat treatment in the normal fashion. Similar, though more complicated, behavior was seen for gallium films. Additional examples such as antimony are discussed in Ref. 76.

The annealing behavior of metal-alloy films is, in general, similar to that of the elemental films discussed above, provided that the composition of the alloys does not differ from the equilibrium values found in bulk. In many cases, however, it is possible to deposit alloy films in which the constituents are present in proportions considerably different from what is thermodynamically permissible. Mader and coworkers<sup>77</sup> have studied a number of such systems. By performing a two-source deposition onto substrates kept at liquid-nitrogen temperature, nonequilibrium compositions were formed by "vapor quenching."

As an example, we may consider the copper-silver system. Figure 29 shows the annealing behavior of a pure silver film as compared with silver films containing 12 and 50% copper, respectively. After deposition at liquid-nitrogen temperature, the films were heated at a constant rate of 30 to 60°C per hour. Surprisingly, the resistivities of all three films as deposited at 80°K were very close to one another. However, the behavior on annealing is seen to be quite different. The pure-metal films show a steep, as well as continuous, decrease in resistivity from 80°K to room temperature.

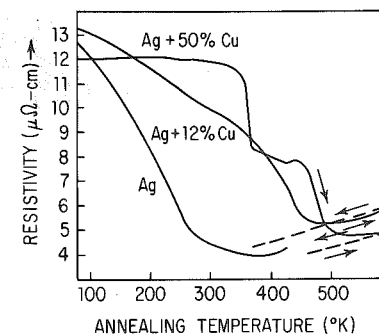


Fig. 29 Annealing behavior of copper-silver alloys of various compositions.

Similar behavior is seen up to 400°K for the films containing 12% copper, although the drop is less steep. These changes appear to be due, as in elemental films, to grain growth and increased perfection. It was concluded that, as deposited, these films are a single, crystalline phase. Similar behavior was seen for alloys containing up to 35% copper. However, upon annealing through the 440 to 480°K range of temperatures, the films changed into a two-phase structure.

Films containing 50% copper were shown to be truly amorphous, as deposited, and the sharp drop in resistivity at approximately 370°K was demonstrated to be due to a transition from the amorphous state to a single, crystalline phase, while the second resistivity drop corresponded to that which was also seen in the more dilute alloys, namely, reversion to a two-phase system. The as-deposited resistivity of the amorphous phase corresponded quite closely to the resistivity of the liquid alloy (extrapolated back to 80°K).

The fact that the alloy containing 50% copper passed through an intermediate stage as a single-phase structure (rather than going directly to the more stable two-phase structure) was explained in terms of the kinetics of the transformation from the amorphous to the crystalline state. This should be more rapid than the transformation to a two-phase structure. Breaking up of the "log jam" present in an amorphous state requires diffusion over only one or two atomic distances. By contrast, the process of segregation into two phases requires relatively long range diffusion.

Early work on the annealing of metal films condensed at liquid-helium temperatures has been reviewed by Neugebauer.<sup>76</sup> Work similar to that reported by Mader has also been done for thin tin films deposited at 20°K and deliberately contaminated with up to 20% copper.

Studies of the annealing characteristics of these metastable-alloy films have also



shown<sup>79</sup> that deposition at a given substrate temperature has considerably more effect on the resistivity of a film than deposition at a lower temperature followed by a subsequent anneal at the higher temperature. For example, films containing 50% copper and 50% silver when deposited at 80°K and then raised to 300°K had a constant resistivity of about 12  $\mu\text{ohm-cm}$ . On the other hand, deposition of the same material at a substrate temperature of 300°K produced a film having a resistivity of only 8  $\mu\text{ohm-cm}$ . This phenomenon is explained as being due to the fact that greater atomic mobility can be achieved during deposition than in the finished film. This is reasonable, since surface diffusion is much greater than bulk diffusion.

Annealing by a somewhat different mechanism can be seen in systems in which an insulating phase is codeposited with the metal. For example, Feldtkeller<sup>80</sup> has studied the annealing of copper films that have been codeposited with SiO. Films were deposited at liquid-helium temperatures, and their resistance was seen to decrease by many orders of magnitude when they were allowed to warm up to 400°K. These results were interpreted as due to the formation of an insulating interface of SiO around the copper grains. As heat treatment proceeded, grain growth of the copper occurred by recrystallization, and the number of grain boundaries became less. The SiO was then squeezed out from between the copper grains into small agglomerates whose influence on the resistivity was small.

In systems where the insulating phase and the metallic phase can chemically react to produce an additional metallic phase, the behavior during annealing is rather different. For example, in the system Cr-SiO, the phase Cr<sub>3</sub>Si is formed during annealing,<sup>81</sup> and far larger proportions of SiO can be tolerated in such films without excessive resistivities after annealing. This is because the Cr<sub>3</sub>Si forms conductive bridges between the chromium crystallites (see also Chap. 18).

#### b. Agglomeration and Oxidation

As was discussed in Chap. 8, during their early stages of growth, thin films consist of individual islands which have many of the characteristics of liquid droplets. As the substrate temperature increases, the contact angle between droplet and substrate decreases and the droplets grow in size. Films deposited at lower temperatures consist of smaller droplets, since the film particles have lower mobility and remain more or less where they land on the substrate. Thus, a given amount of material deposited on a substrate at a low temperature may be enough to form a continuous film, whereas the same amount of material deposited on a hotter substrate will result in an island structure.

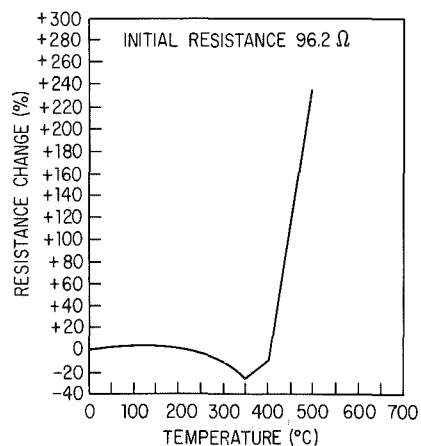


Fig. 30 Resistance vs. temperature for a thin film showing sudden irreversible increase associated with agglomeration.

Because of this phenomenon, it is found that very thin films (in the order of a few hundred angstroms, or less) which possess a continuous structure at their deposition temperature will, when heat-treated, revert to an island structure. This process is referred to as agglomeration and is easily detected by the large increase in resistance that occurs if the film is subjected to too high a temperature. An example is shown in Fig. 30 (taken from Ref. 82). For a given substrate-material combination, there is thus a definite lower limit to the thickness of thin films that are capable of standing up to a given amount of heat treatment. Belser and Hicklin<sup>82</sup> have listed the limits of sheet resistance for various metal films that could survive temperature cycling to 600°C. These vary from a few ohms per square for gold films to more than 4,000 ohms/sq for tungsten films.

Since agglomeration occurs rather suddenly, and since it is associated with a loss of desirable properties, only a few quantitative observations of agglomeration have been reported. In one such study of gold films on zinc sulfide substrates,<sup>83</sup> agglomeration is pictured as occurring in three stages. Initially, small holes are formed in the films, the holes then enlarge, and finally the film separates into islands. The observed resistance changes occur primarily during the second and third stages. It was concluded that the process is a thermally activated one associated with the migration of gold atoms. For this particular system, an activation energy of 1.8 eV was measured.

Skofronick and Phillips<sup>84</sup> have studied the incidence of additional agglomeration in films that, as deposited, are already discontinuous. In films deposited at 90°K and then warmed to room temperature, the resistance first decreased slightly and then increased irreversibly by several orders of magnitude. The model which they invoked to explain the observed behavior was that the effect of heat treatment was to cause motion of the smaller islands, which then coalesced with the larger ones. The mobility of the islands on the substrates and the number of islands with sufficient energy to move are determined by an assumed thermally activated process. As the islands combine, the mean gap between them increases. A typical activation energy was of the order of 0.2 eV. It was also shown that the influence on the results of thermal expansion of the substrate was negligible.

Unless they are suitably protected, many thin films when heated in air undergo increases in resistance because of oxidation. Ultimately they may be converted to insulating films if the treatment is carried on long enough. It has been found that the increase in the resistance of a film is considerably greater than can be accounted for on the basis of only the reduced thickness of the conductive portion of the film resulting from oxidation of the surface. Quantitative evidence for this has been provided by Basseches in a study of the oxidation of tantalum films.<sup>64</sup> He suggested that the oxidation was occurring along the grain boundaries of the films, a hypothesis that had also been advanced to explain the oxidation of iron films.<sup>85</sup> Confirmation of this concept was later obtained by Maissel,<sup>63</sup> who showed that the oxidation of the grain boundaries could occur either as a result of oxygen diffusing in from the surface or from trapped oxygen diffusing internally and then precipitating at the grain boundaries as an insulating phase. The progress of grain-boundary oxidation was correlated with the high-frequency characteristics of the film. It seems likely that these results for tantalum films can be generalized for most other films.

It is interesting to note that even though the change in resistance that occurs during oxidation is much greater than can be accounted for from the equilibrium thickness of oxide at the surface, the actual thickness of the oxide on the surface appears to be less than the corresponding thickness in bulk material, at least for the case of tantalum.<sup>86</sup> The effect is not understood, and it is speculated that it might be due to the known lack of crystallinity of the oxides of thin films deposited on smooth substrates. The fact that the film was even thinner than the usual value furthers the important role of grain-boundary oxidation.

In the case of alloy films, it is possible for preferential oxidation of one of the components to occur. For example, it has been shown<sup>87</sup> that alloy films of the Chromel family (containing nickel, chromium, and iron) exhibit a complicated resistance vs. time curve when heat-treated in air. Initially, the resistance of the film increases with time because of the oxidation of the iron. However, once oxidation of this component is complete, the effect of annealing of defects becomes more important and the resistance begins to decrease with time. Finally, the resistance begins to increase once more as the major fraction of the defects has been annealed out, and the dominant contribution to further change comes from oxidation of the chromium and nickel constituents.

#### REFERENCES

1. Wilson, A. H., "The Theory of Metals," Cambridge University Press, New York, 1958.

2. Mott, N. F., and H. Jones, "The Theory of the Properties of Metals and Alloys," Dover Publications, Inc., New York, 1958.
3. Bardeen, J., *J. Appl. Phys.*, **11**, 88 (1939).
4. Linde, J. O., *Ann. Physik*, **15**, 239 (1932).
5. Gerstenberg, D., and C. J. Calbick, *J. Appl. Phys.*, **35**, 402 (1964).
6. Damask, A. C., and G. J. Dienes, "Point Defect in Metals," Gordon and Breach, Science Publishers, Inc., New York, 1963.
7. Reale, C., *Phys. Letters*, **2**, 268 (1962).
8. Overhauser, A. W., and R. L. Gorman, *Phys. Rev.*, **102**, 676 (1956).
9. Ziman, J. M., "Electrons and Phonons," p. 237, Oxford University Press, Fair Lawn, N.J., 1960.
10. Blewitt, T. H., R. R. Coltman, and J. K. Redman, *Phys. Rev.*, **93**, 118 (1937).
11. Krantz, E., and H. Schultz, *Z. Naturforsch.*, **9a**, 125 (1954).
12. Altman, C., *Proc. 9th Natl. Vacuum Symp.*, 1962, p. 174.
13. Young, I. G., and C. W. Lewis, *Proc. 10th Natl. Vacuum Symp.*, 1963, p. 428.
14. Valdes, L. B., *Proc. IRE*, **42**, 420 (1954).
15. Logan, M. A., *Bell System Tech. J.*, **40**, 885 (1961).
16. Smits, F. M., *Bell System Tech. J.*, **37**, 699 (1958).
17. Zrudsky, D. R., H. D. Bush, and J. R. Fassett, *Rev. Sci. Instr.*, **37**, 885 (1966).
18. Thomson, J. J., *Proc. Cambridge Phil. Soc.*, **11**, 120 (1901).
19. Fuchs, K., *Proc. Cambridge Phil. Soc.*, **34**, 100 (1938).
20. Sondheimer, E. H., *Advan. Phys.*, **1**, 1 (1952).
21. Campbell, D. S., "The Use of Thin Films in Physical Investigations," p. 299, Academic Press Inc., New York, 1966.
22. Dekker, A. J., "Solid State Physics," Prentice-Hall, Inc., Englewood Cliffs, N.J., 1957.
23. Mayer, H., "Structure and Properties of Thin Films," p. 225, John Wiley & Sons, Inc., New York, 1959.
24. Mayer, H., "Physik duenner Schichten," vol. 2, Wissenschaftliche Verlagsgesellschaft m.b.H., Stuttgart, 1955.
25. Worden, D. G., and G. C. Danielson, *J. Phys. Chem. Solids*, **6**, 89 (1958).
26. Nossek, R., "Basic Problems in Thin Films Physics," p. 550, Vandenhoeck and Ruprecht, Goettingen, 1966.
27. Parrott, J. E., *Proc. Phys. Soc., London*, **85**, 1143 (1965).
28. Chopra, K. L., *Phys. Rev.*, **155**, 660 (1967).
29. Abeles, F., and M. L. Theye, *Phys. Letters*, **4**, 348 (1963).
30. Cirkler, W., *Z. Physik*, **147**, 481 (1957).
31. Gillham, E. J., J. S. Preston, and B. E. Williams, *Phil. Mag.*, **46**, 1051 (1955).
32. Ennos, A., *Brit. J. Appl. Phys.*, **8**, 113 (1957).
33. Chopra, K. L., and L. C. Bobb, *Acta Met.*, **12**, 807 (1964).
34. Lucas, M. S. P., *Appl. Phys., Letters*, **4**, 73 (1964).
35. Chopra, K. L., and M. R. Randlett, *J. Appl. Phys.*, **38**, 3144 (1967).
36. Suhrmann, R., *Advan. Catalysis*, **7**, 303 (1955).
37. Swietering, R., H. L. T. Koks, and C. VanHeerden, *J. Phys. Chem. Solids*, **11**, 18 (1959).
38. Komnik, Yu F., and L. S. Palatnik, *Soviet Phys. Solid State*, **7**, 429 (1965).
39. Drumheller, C. E., *Proc. 4th Natl. Vacuum Symp.*, 1957, p. 27.
40. Andrews, E. R., *Proc. Phys. Soc. London*, **A62**, 77 (1949).
41. Sondheimer, E. H., *Phys. Rev.*, **80**, 401 (1950).
42. Jeppesen, M. A., *J. Appl. Phys.*, **37**, 1940 (1966).
43. Forsvoll, K., and I. Holwech, *Phil. Mag.*, **9**, 435 (1964).
44. Forsvoll, K., and I. Holwech, *Phil. Mag.*, **10**, 921 (1964).
45. Chopra, K. L., and S. K. Bahl, *J. Appl. Phys.*, **38**, 3637 (1967).
46. MacDonald, D. K. C., and K. Sarginson, *Proc. Roy. Soc. London*, **A203**, 223 (1950).
47. Holwech, I., *Phil. Mag.*, **12**, 117 (1965).
48. Neugebauer, C. A., and R. H. Wilson, "Basic Problems in Thin Film Physics," p. 579, Vandenhoeck and Ruprecht, Goettingen, 1966.
49. Mostovetch, N., and B. Vodar, "Semiconducting Materials," p. 260, Butterworth & Co. (Publishers), Ltd., London, 1951.
50. Minn, S. S., *J. Rech. Centre Natl. Rech. Sci. Lab. Bellevue Paris*, **51**, 131 (1960).
51. Neugebauer, C. A., and M. B. Webb, *J. Appl. Phys.*, **33**, 74 (1962).
52. Hill, R. M., *Nature*, **204**, 35 (1964).
53. Neugebauer, C. A., *Proc. 9th Natl. Vacuum Symp.*, 1962, p. 45.
54. Hill, R. M., *Thin Solid Films*, **1**, 39, 1967.
55. Skofronick, J. G., W. B. Phillips, K. T. McArdle, and R. H. Davis, *Bull. Am. Phys. Soc.*, **10**, 364, 1965.

56. Gorter, C. J., *Physica*, **17**, 778 (1950).
57. Darmois, E., *J. Phys. Radium*, **17**, 210 (1956).
58. Hartman, T. E., *J. Appl. Phys.*, **34**, 943 (1963).
59. Herman, E. S., and T. N. Rhodin, *J. Appl. Phys.*, **27**, 1594 (1966).
60. Feldman, C., *J. Appl. Phys.*, **34**, 1710 (1963).
61. Milgram, A. A., and C. Lu, *J. Appl. Phys.*, **37**, 4773 (1966).
62. Maissel, L. I., and P. M. Schaible, *J. Appl. Phys.*, **36**, 237 (1965).
63. Maissel, L. I., *Proc. 9th Natl. Vacuum Symp.*, 1962, p. 169.
64. Basseches, H., *IRE Trans. Component Pts.*, **CP8**, 51 (1961).
65. Offret, M., and M. D. Vodar, *J. Phys. Radium*, **17**, 237 (1955).
66. Howe, G. W. O., *Wireless Eng.*, **12**, 291 (1935).
67. Howe, G. W. O., *Wireless Eng.*, **17**, 471 (1940).
68. Humphrey, J. N., F. L. Lummis, and W. W. Scanlon, *Phys. Rev.*, **90**, 11 (1953).
69. Primak, W., *Phys. Rev.*, **100**, 1677 (1955).
70. Vand, V., *Proc. Phys. Soc. London*, **55**, 222 (1943).
71. Wilkinson, P. G., and L. S. Birks, *J. Appl. Phys.*, **20**, 1168 (1949).
72. Wilkinson, P. G., *J. Appl. Phys.*, **22**, 419 (1951).
73. Troyoda, H., and M. Nagashima, *J. Phys. Soc. Japan*, **14**, 274 (1959).
74. Hoffman, R. W., F. J. Anders, and E. C. Crittenden, Jr., *J. Appl. Phys.*, **24**, 231 (1953).
75. Buckel, W., and R. Hilsch, *Z. Physik*, **138**, 109 (1954).
76. Neugebauer, C. A., "Physics of Thin Films," vol. 2, p. 1, Academic Press Inc., New York, 1964.
77. Mader, S., A. S. Nowick, and H. Widmer, *Acta Met.*, **15**, 203 (1967).
78. Ruhl, W., *Z. Physik*, **138**, 121 (1954).
79. Nowick, A. S., and S. Mader, Basic Problems in Thin Film Physics, *Proc. Intern. Symp.*, 1966, p. 212, Vandenhoeck and Ruprecht, Clausthal.
80. Feldtkeller, E., *Z. Physik*, **157**, 65 (1959).
81. Glang, R., R. Holmwood, and S. Herd, *J. Vacuum Sci. Technol.*, **4**, 163 (1967).
82. Belser, R. B., and W. H. Hicklin, *J. Appl. Phys.*, **30**, 313 (1959).
83. Kane, W. M., J. P. Spratt, and L. W. Hershinger, *J. Appl. Phys.*, **36**, 2085 (1966).
84. Skofronick, J. E., and W. B. Phillips, *Proc. Intern. Symp.*, 1966, p. 591, Vandenhoeck and Ruprecht, Clausthal.
85. VanItterbeek, A., L. DeGreve, and M. Francois, *Med. Koninkl. Vlaam. (Acad. Wetens. Belg. Klasse Wetenschap*, 1950), vol. 12, p. 3.
86. Basseches, H., *J. Electrochem. Soc.*, **109**, 475 (1962).
87. Dean, E. R., *J. Appl. Phys.*, **35**, 2930 (1964).